"Original contains color plates: All DTIC reproductions will be in black and white"

SECURITY CLASSIFICATION OF THIS PAGE

AD-A241 481

DTIC ELECTE OCT 1 1991 S C D

1a. REPORT SECURITY CLASSIFICATION U	1b. RESTRICTIVE MARKINGS N/A
2a. SECURITY CLASSIFICATION AUTHORITY N/A	3. DISTRIBUTION/AVAILABILITY OF REPORT Distribution Unlimited
2b. DECLASSIFICATION/DOWNGRADING SCHEDULE N/A	
4. PERFORMING ORGANIZATION REPORT NUMBER(S) N/A	5. MONITORING ORGANIZATION REPORT NUMBER(S)
6a. NAME OF PERFORMING ORGANIZATION Argonne National Laboratory	6b. OFFICE SYMBOL (If applicable) N/A
7a. NAME OF MONITORING ORGANIZATION Office of Naval Research	
6c. ADDRESS (City, State, and ZIP Code) 9700 S. Cass Avenue Argonne, IL 60439	7b. ADDRESS (City, State, and ZIP Code) 800 N. Quincy Street Arlington, VA 22217-5000
8a. NAME OF FUNDING/SPONSORING ORGANIZATION Defense Initiative Org.	8b. OFFICE SYMBOL (If applicable)
9. PROCUREMENT INSTRUMENT IDENTIFICATION NUMBER N00014-87-F-0022	
8c. ADDRESS (City, State, and ZIP Code) Washington, DC 20301-7100	10 SOURCE OF FUNDING NUMBERS PROGRAM ELEMENT NO. / PROJECT NO. / TASK NO. / WORK UNIT ACCESSION NO.

11. TITLE (Include Security Classification)
(U) Sofe X-Ray Undulator Final Report

12. PERSONAL AUTHOR(S)
Samuel D. Bader

13a. TYPE OF REPORT	13b. TIME COVERED	14. DATE OF REPORT (Year, Month, Day)	15. PAGE COUNT
Final	FROM 3/90 TO 9/91	1991, 09, 24	

16. SUPPLEMENTARY NOTATION
Final Activities Report

17. COSATI CODES		
FIELD	GROUP	SUB-GROUP

18. SUBJECT TERMS (Continue on reverse if necessary and identify by block number)
Soft X-Ray Undulator
Synchrotron-Radiation Source
Insertion Device

19. ABSTRACT (Continue on reverse if necessary and identify by block number)

A soft x-ray undulator has been based at the vacuum ultraviolet storage ring at the National Synchrotron Light Source. The undulator is being used as a radiation source by a multi-institutional research team to perform the first spin-polarized photoemission experiments in the United States to study novel ultrathin magnetic films and surfaces.

91-12008

20. DISTRIBUTION/AVAILABILITY OF ABSTRACT	21. ABSTRACT SECURITY CLASSIFICATION	
☐ UNCLASSIFIED/UNLIMITED ☐ SAME AS RPT. ☐ DTIC USERS		
22a. NAME OF RESPONSIBLE INDIVIDUAL M. Marron	22b. TELEPHONE (Include Area Code) 202-696-4083	22c. OFFICE SYMBOL ONR

DD FORM 1473, 84 MAR — 83 APR edition may be used until exhausted. All other editions are obsolete.

SECURITY CLASSIFICATION OF THIS PAGE

91 9 30 180

AD NUMBER	DATE	DTIC ACCESSION NOTICE
	9/24/91	

1. REPORT IDENTIFYING INFORMATION

A. ORIGINATING AGENCY

Argonne National Laboratory

B. REPORT TITLE AND/OR NUMBER

Soft X-Ray Undulator Final Report

C. MONITOR REPORT NUMBER

D. PREPARED UNDER CONTRACT NUMBER

N00014-87-F-0022

2. DISTRIBUTION STATEMENT

Distribution Unlimited

REQUESTER:

1. *Put your mailing address on reverse of form.*
2. *Complete items 1 and 2.*
3. *Attach form to reports mailed to DTIC.*
4. *Use unclassifed information only.*

DTIC:

1. *Assign AD Number.*
2. *Return to requester.*

FORM DTIC 50 DEC 80 *U.S. GPO: 1982-381-508/1392 PREVIOUS EDITIONS ARE OBSOLETE

S.D. Bader
Materials Science Division
Building 223
Argonne National Laboratory
9700 S. Cass Ave.
Argonne, IL 60439

FINAL REPORT

March 1990 - September 1991

SOFT X-RAY UNDULATOR

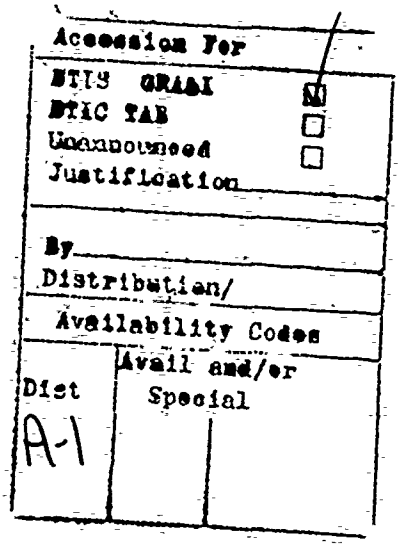

S. D. Bader

Materials Science Division

Argonne National Laboratory

Argonne, Illinois 60439

Office of Naval Research Contract #N00014-87-F-0022

MFEL Program

Strategic Defense Initiative Organization

This is the Final report for the program to base a soft x-ray undulator at the vacuum ultra-violet (VUV) storage ring at the National Synchrotron Light Source (NSLS). The undulator is being used as a radiation source by multi-institutional research teams to perform pioneering spin-polarized photoemission experiments. The undulator source provides major opportunities in materials research in the forefront area of ultrathin magnetic films and surfaces. In the present report the history of the project is summarized and the successful outcome is documented.

An undulator was designed at ANL that was meant to serve multiple needs. Firstly, the SDIO MFEL program was mandated to establish regional facilities to advance the utilization of tunable radiation sources. While our project at NSLS involves synchrotron radiation, as opposed to free-electron laser radiation, FEL sources that operate in the soft-x-ray and VUV region (XUV) are still considered futuristic. Undulators, on the other hand, provide tunable, *laser-like* radiation, and can be used to prepare a community of researchers to utilize XUV FEL sources when they become more generally available. Secondly, a multi-institutional group of investigators was already organized at the time, under the aegis of the National Science Foundation (NSF) Materials Research Group (MRG) program, for the purpose of advancing the state-of-the-art in fundamental research in magnetic materials by utilizing a new radiation source to perform the first spin-polarized photoemission experiments in the United States. The MRG continues to flourish and involves a number of distinguished U.S. researchers at national laboratories, universities and industry. The materials of interest to the MRG involve magnetic surfaces, films and interfaces, including artificially layered structures with novel properties and applications. The case for involvement in such magnetic materials-research activities has been documented repeatedly, especially because of the need to improve the U.S. economic outlook with respect to high-tech opportunities. Finally, the undulator development project provided Argonne National Laboratory (ANL) with an opportunity to do generic design work related to future insertion devices for its new 7-GeV synchrotron storage ring called the Advanced Photon Source

(APS) which is presently under construction. These three motivating factors were the underpinnings of a successful project. There was national and local interest in the project and there was the desire to take the lead internationally in the fields of interest. And most importantly, sufficient funding as well as talent was allotted to the project. The undulator that has resulted from our efforts has not been officially named, but it is often referred to as the U5 undulator, since it serves the U5 beamline at NSLS.

The process of developing the undulator involved a complex series of design and procurement steps. The magnetic-lattice design decided upon utilizes a Halbachian hybrid structure consisting of Nd-Fe-B permanent magnets and vanadium permendur pole pieces. There are 27 periods (54 poles) and a period length of 7.5 cm. This design configuration and the magnetic and mechanical tolerances were set at ANL.[1] Specifications for outside procurement and a schedule of design reviews also were established by the ANL procurement team. The mechanical and magnet end-corrector designs, and engineering and construction work was then contracted out to Spectra Technology, Inc. of Bellevue, Washington, after a prolonged open-bidding process. [Incidentally, Spectra Technology was, at the time of procurement, a subsidiary of Spectra Physics, then became an Amoco company, and, most recently has changed names to STI Optronics.] Consultants from NSLS and from the Advanced Light Source at Lawrence Berkeley Laboratory were included in the formulation and review of the commercial package. The central aspect of the mechanical design was a computer-controlled, variable-gap mechanism to change the peak magnetic field, and, thus, to tune the photon energy and harmonic content of the resultant undulator radiation. The goal was to utilize the high-brilliance of the first and third harmonics to cover the desired photon-energy range of ~15-150 eV. The range was dictated by the needs of the experimental photoemission program. Given the constraint of

---

1. P.J. Viccaro, G.K. Shenoy, S.H. Kim and S.D. Bader, "Soft x-ray undulator for the U5 beamline at NSLS", Rev .Sci. Instrum. **60**, 1813 (1989).

the storage-ring energy of 0.75 GeV, a maximum field of ~4.6 kG at the minimum gap setting of 3.4 cm. was needed and was achieved.

An independent aspect of the project involved redesigning and equipping the vacuum section of the storage ring on which the undulator was to be mounted. The construction, conditioning and installation tasks associated with the new vacuum chamber were contracted out to NSLS, and the hardware (gate valves, pumps, gauges, controllers, etc.) was purchased at ANL. NSLS kindly agreed to participate in the project by taking care of the installation and surveying in-place of the massive undulator. The vacuum-design activities led to sponsorship of a conference on the "Vacuum Design of Synchrotron Light Sources" at ANL, the proceedings of which should serve the community at large well into the future.[2]

The undulator was installed in May of 1990. It has met and generally surpassed all design criteria set for its performance. It is now acknowledged as a world-class device that sets a new design standard for future insertion devices. It meets the demanding tolerance requirements for insertion devices at the APS,[3] and, if installed on the appropriate accelerator or storage ring, it should perform as a free-electron laser. Figure 1 shows an intensity spectrum of the undulator at a fixed-gap setting that is closed around the vacuum chamber. Note the rich definition in the harmonic content, and the structure that extends out to even the seventh harmonic at ~140-eV photon energy. This data was taken early on in the commissioning process. Other spectra appear in Appendices I and III of this document.

---

2. Vacuum Design of Synchrotron Light Sources, AIP Conf. Proc. No. **236**, American Vacuum Society Series 12, edited by Y. G. Amer, S.D. Bader, A. R. Krauss, and R. C. Neimann (AIP, New York, 1991) 428 pages.

3. J. Viccaro and E. Gluskin, "An APS Prototype Undulator at NSLS", in Advanced Photon Source User Update, Issue No. 2, April 1991, pp.17-18.

The final stage of the undulator development project involved a comprehensive characterization of the device. Magnetic and mechanical tolerance measurements were performed at Spectra Tech and at NSLS before installation on the VUV ring. These measurements serve as the basis for some of the performance claims. But the ultimate test involves the quality of the radiation the device produces at the U5 endstation. Toward the end of providing the necessary characterization, an ambitious effort was undertaken to measure the polarization of the undulator radiation. A unique XUV polarimeter[4] was designed at ANL for the task under the leadership of E. Gluskin, an XUV expert, formerly at the Novosibirsk synchrotron in the USSR.[5] Also, John Mattson, an MRG post-doc, was hired in Sept. 1990 and has been resident at ANL to work on the polarimeter and to serve as liason to the beamline at NSLS.

The polarimeter uses a set of five different Mo/Si multilayer mirrors, each one of which is matched to a harmonic of the undulator when its gap is closed around the vacuum chamber. The multilayers serve as Bragg-reflectors, and are set at the Brewster's angle (45°) to pass only *s*-polarized light. The mirror and detector assembly can be rotated 180° (as shown schematically in Fig. 4 of Appendix I) to measure the *s*-component of the light in all directions. The polarimeter is set on a five-axis goniometer. Each of the multilayers can be translated in place without breaking vacuum. Pinholes of variable size also can be translated in front of the multilayers to provide spatial definition. Figure 7 of Appendix I shows scans of the polarization of the fourth-harmonic radiation at ~75 eV. The on-axis

---

4. E. S. Gluskin, J.E. Mattson, S.D. Bader, P.J. Viccaro, T.W. Barbee, Jr., N.B. Brookes, A. Pitas, and R. Watts, "XUV polarimeter for undulator radiation measurements", submitted to SPIE Conf., San Diego, July 21-26, 1991.

5. E. S. Gluskin, S.V. Gaponov, P. Dhez, P.P. Ilinsky, N.N. Salashchenko, Y.M. Shatunov, and E.M. Trakhtenberg, "A polarimeter for soft x-ray and VUV radiation", Nucl. Instrum. Methods A246, 394 (1986).

data shows the expected $\cos^2\theta$-behavior for radiation linearly polarized in the plane of the storage ring. The off-axis data, however, shows a background signal that appears most noticably as 'wings' in the curve at high angles. This indicates the presence of an unpolarized or elliptically polarized radiation component. This is an exciting, new result that is unexpected based on results of standard simulation codes that utilize the 'far-field' approximation. Although these are our first results, the synchrotron-radiation community at large is quite interested in XUV polarimetry. This is because of a desire to realize insertion devices dedicated to producing variable-ellipticity radiation by utilizing advanced concepts, such as crossed or helical undulators, or asymmetric wigglers.

Thus, the undulator project has been highly successful for all concerned. ANL has commissioned a state-of-the-art device for use in the spin-polarized-photoemission program at NSLS, and the field of synchrotron radiation, in general, has been advanced in a number of ways. In addition, active contact was made with a segment of the FEL community when I served in June, 1990 as member of the Review and Advisory Committee for a Los Alamos XUV-IR FEL National Users Facility preproposal. Most importantly, a domestic supplier of undulators has been nurtured and our undulator serves as its model of achievement, as shown in the advertisement that appears as AppendixV of this document.[6]

---

6. Synchrotron Radiation News, Vol. 4, No. 4 (1991) p. 28.

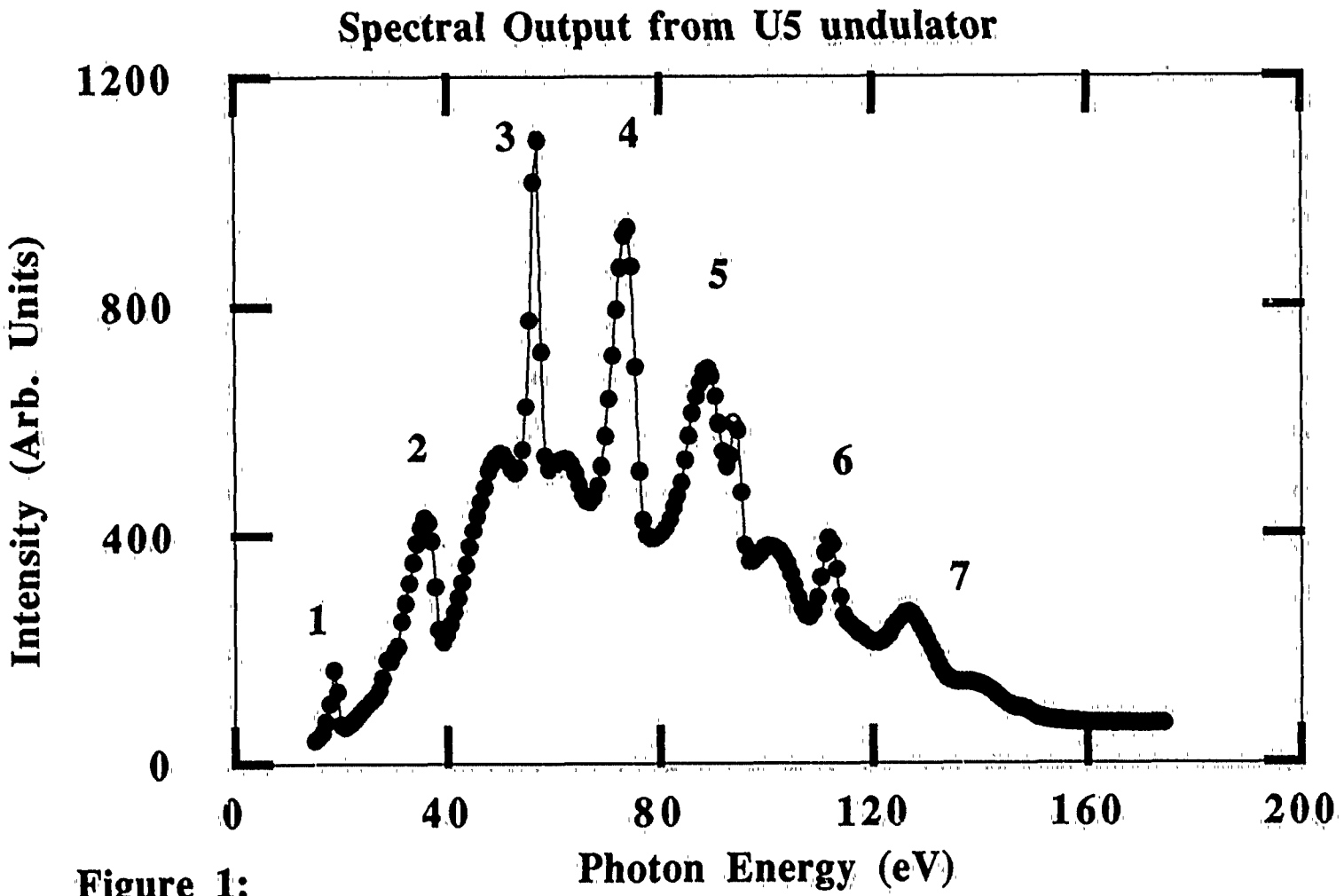

Figure 1:

Spectrum from the U5 undulator that is collected by measuring the photocurrent from the sample in the experimental chamber. The undulator gap was set to 3.2 cm.

Appendices:

I. Preprint:

E. S. Gluskin, J.E. Mattson, S.D. Bader, P.J. Viccaro, T.W. Barbee, Jr., N.B. Brookes, A. Pitas, and R. Watts, "XUV polarimeter for undulator radiation measurements", submitted to SPIE Conf., San Diego, July 21-26, 1991.

II. Some preprints and reprints of spin-polarized photoemission research using the U5 undulator:

A. Comment on "Direct Observation of Spin-Split Electronic States of Pd at the Pd(111)/Fe(110) Interface", Y. Chang, N. B. Brookes, P. D. Johnson, and S. D. Bader, Phys. Rev. Lett. (submitted).

B. "Magnetic Interface States and Finite-Size Effects", N. B. Brookes, Y. Chang, P. D. Johnson, and S. D. Bader, Phys. Rev. Lett. **67**, 354 (1991).

C. "Spin Polarized Photoemission Studies of Surfaces and Thin Films", P. D. Johnson, N. B. Brookes, Y. Chang, Materials Research Society Proceedings (1991) in press.

III. Copy of :

J. Viccaro and E. Gluskin, "An APS Prototype Undulator at NSLS", in Advanced Photon Source User Update, Issue No. 2, April 1991, pp.17-18.

IV. Table of Contents of Conference held at ANL:

Vacuum Design of Synchrotron Light Sources, AIP Conf. Proc. No. **236**, American Vacuum Society Series 12, edited by Y. G. Amer, S.D. Bader, A. R. Krauss, and R. C. Neimann (AIP, New York, 1991) 428 pages.

V. Advertisement of commercial undulator that appeared in:

Synchrotron Radiation News, Vol. **4**, No. 4 (1991) p. 28.

VI. "Studio portrait" glossy photo of U5 undulator.

XUV Polarimeter for undulator radiation measurements

E. Gluskin, J. E. Mattson, S.D. Bader, P.J. Viccaro,
Argonne National Laboratory

T.W. Barbee, Jr,
Lawrence Livermore National Laboratory

N. B. Brookes, Brookhaven National Laboratory

A. Pitas, Baker Manufacturing Co. WI

R. Watts, National Institute of Standards and Technology

ABSTRACT

A polarimeter for x-ray and vacuum ultraviolet (XUV) radiation was built to measure the spatial and spectral dependence of the polarization of the light produced by the new undulator at the U5 beamline at NSLS. The fourth-harmonic radiation was measured, and it does not agree with predictions based on ideal simulation codes in the far-field approximation.

INTRODUCTION

The availability of sychrotron radiation has had a dramatic impact on a diverse array of multidisciplinary spectroscopies. In recent years the variability of the polarization of synchrotron radiation has been utilized in widespread applications,[1,2,3] including spin-polarized photoemission, inverse photoemission, circular dichroism, *etc.* The gathering and interpretation of such measurements are greatly simplified by taking advantage of the polarization properties of synchrotron sources. This is

especially the case for the latest generation of undulator- and wiggler-based experiments. However, the approach suffers from the fact that the actual spatial and spectral distribution of polarization states of a given source has rarely been measured. Rather, the procedure has been that each experimentalist is forced to rely on the polarization properties calculated for an "ideal" source. But, the calculations are limited in their accuracy largely because of both the finite beam emittance of the source, and the presence of random errors in the magnetic profiles of the insertion device. These factors can significantly alter the polarization. Therefore, as the need for polarized-light sources increases, there is a concomitant need for accurate measurements of the polarization over a wide spectral range.

Recently considerable developmental work[7,8,9] has been devoted to polarization measurements for soft x-ray and vacuum ultraviolet (VUV) synchrotron radiation. The first soft x-ray polarimeter was developed by Gluskin, *et al.* to measure the radiation from a helical undulator.[10] The aim of the present work is the development of an advanced polarimeter to characterize the polarization of the radiation from the new undulator recently installed at the U5 beamline on the VUV-ring at the National Synchrotron Light Source (NSLS) at Brookhaven National Laboratory. The radiation from the U5 undulator is used for spin-polarized photoemission experiments. In these experiments undulator radiation is needed to partially compensate for the known inefficiencies of the electron spin detectors.

EXPERIMENTAL BACKGROUND

The U5 undulator is a planar insertion device with the following parameters:[11]

Undulator Period	λ_u = 7.5 cm
Number of Period	n = 27
Deflection parameter	K = 2.3
Distance	
Undulator to Pinhole	5.4 m
Pinhole to polarimeter	1.7 m

The K-value is actually variable, but for the present work it was fixed at the above value. The undulator is a hybrid design based on Nd-Fe-B permanent magnets and vanadium permendur pole pieces.

The polarization measurements were performed by the polarimeter schematically shown on Fig. 4. The polarimeter consists of five sets of Mo/Si multilayer polarizers placed in the ultrahigh vacuum (UHV) chamber and supported by a 5-axis goniometer assembly. These polarizers take advantage of the property that metals have an index of refraction $n \approx 1$ for photon energies above ~58 eV, and, thus, have a Brewster's angle of 45°. Additionally, by designing the polarizers as multilayer structures one can selectively enhance a particular wavelength with the proper choice of the multilayer period. Then, by placing a polarizer at 45° with respect to the incident beam one simply has to measure the intensity of the reflected light to measure the *s*-polarized component of the incident light (scaled by the reflectivity of the multilayer). By rotating this assembly over 180° one can measure all the linear polarized components of the incident light. Note that there is one limitation to this method which is that circular and non-polarized light cannot be distinguished without separate measurements utilizing the equivalent of a quarter-wave plate.

Five different Mo/Si multilayer Bragg-reflectors were used as polarizers for the energy region 58-98 eV. Each was designed to have its maximum reflectivity at an angle of incidence of 45° for a different specific energy range that encompassed that of the first five harmonics of the undulator. Further, the polarimeter design permits the positioning of any of the five multilayers onto the analyzed beam without breaking vacuum.

Mechanical adjustments provide the ability to align the polarizer axis of rotation parallel to the incident beam axis to within 0.1-mrad accuracy. These adjustments also allow us to translate the polarimeter with respect to the beam center with a 10-μ accuracy. The rotation of the polarizer/detector assembly is controlled to within a 0.1° accuracy. An illuminated area of 25x25 mm can be analyzed with the spatial resolution

of 0.01 mm by means of one of three different pinholes on the polarimeter. A GaAs Schottky diode with an active area of 5x5 mm or a UDT Si diode with a 10x10-mm active area were used as detectors because of their spatial uniformity and sensitivity.

RESULTS

Energy spectra will be presented first and then the polarization information will be presented. A typical energy spectrum from the U5 undulator is shown on Fig. 1. The spectrum was measured with a 1-mm diameter pinhole placed on the center of the irradiated area (see Fig. 2). The spectrum was collected by measuring the photocurrent from a Ni target, and was not normalized to take into account the quantum efficiency of Ni. The ratio of intensities between the wide and narrow parts of the fifth harmonic located between 90-100 eV is not reproduced in the computer simulations.

Next the energy dependence of the radiation was measured for various horizontal displacements of the pinhole in the plane of the storage ring. Three of these spectra are shown in Fig. 3. From these spectra we see a strong left-right asymmetry in the radiation emitted from the U5 undulator. This asymmetry is not present in calculated spectra using present-day algorithms. These types of measurements confirm the need for comprehensive experimental characterizations of undulator sources.

For the polarization measurements five multilayers were chosen to span the energy region of the undulator harmonics. Spectral reflectivity measurements of the polarizers were performed at the SURF II beamline at NIST.[13] The results for two of the polarizers are shown superimposed with measurements of the undulator spectra in Fig. 5. The polarization measurements were conducted by first rotating the analyzer/detector assembly of the polarimeter to the position shown schematically in Fig. 4b. This position is designated as -90°. In this configuration the detected beam is completely polarized perpendicular to the plane of the storage ring. Then the intensity measured by the detector is recorded as the assembly is rotated by 180° to the +90° position. A typical scan is shown in Fig. 6.

The data show the expected fit to a $\cos^2(\theta)$ angular dependence (the solid line). A series of such scans were performed for different vertical positions by translating the polarimeter above or below the plane of the storage ring. Two of these scans are shown in Fig. 7. The data were taken using the multilayer which selected out the fourth-harmonic radiation at ~75 eV. The unusual feature to focus on is that the off-axis data in Fig. 7 appears to be superimposed on a background signal; this produces the wings at high angles compared to the on-axis data. The shape of the curve indicates that the off-axis light either becomes elliptical or includes an unpolarized component. While we cannot distinguish between the two possibilities, neither are predicted by the ideal simulation codes.

CONCLUSION

In summary we have built and tested a XUV polarimeter capable of measuring the polarization from VUV and soft X-ray synchrotron sources, including insertion devices. Our first measurements of the polarization of the U5 undulator at NSLS indicate that there are significant contributions to the light that cannot be explained with calculations that use the "far-field" approximation. This has significant implications for the characterization and utilization of the new types of insertion devices, such as helical or crossed undulators, and asymmetric wigglers, that are being developed exclusively for the production of variable polarization radiation.

ACKNOWLEDGEMENTS

This work is sponsored by the U.S. Department of Energy, BES-Materials Sciences under contract W-31-109-ENG-38. J.E.M. and N.B.B. were supported by the NSF MRG Contract No. DMR-86-03304.

References

1. E.W. Plummer and W. Eberhardt, in Advances in Chemical Physics, **49**, 553 (1982)

2. P.D.Johnson, A. Clarke, N.B. Brookes, S.L. Hulbert, B. Sinkovic and N.V. Smith, Phys.Rev.Lett. **61**, 2257 (1988)
3. D.M. Mills, SPIE **1345**, 125 (1990)
4. H. Onuki, Nucl. Instr. Meth. **A246**, 94 (1986)
5. P. Elleaume, "ESRF Internal Report", ESRF-SR/1D-88-23
6. K.-J. Kim, Nucl. Instr. Meth **219**, 425 (1984)
7. A. Gaupp and M. Mast, Rev. Sci. Instrum. **60**(7), 2213 (1989)
8. P. Dhez, Nucl. Instr. Meth. **A261**, 66 (1987)
9. T. Koide and T. Shidara, to be published Appl. Phys. Lett., June 1991
10. E.S. Gluskin, S.V. Gaponov *et al.*, Nucl. Instr. Meth. **A246**, 394 (1986)
11. P.J. Vicarro, G.K. Shenoy, S.H. Kim and S.D. Bader, Rev. Sci. Instrum. **60**, 1813 (1989)
12. P.D. Johnson, S.L. Hulbert, *et. al.* , submitted to Rev. Sci. Instru.
13. J.R. Roberts, J. Kerner and G.B. Salomon, Physica Scripta **41**, 9 (1990)

Figure Captions

Figure 1. Typical spectrum from U5 undulator. Measurements were taken with 1-mm pinhole at the center of the photon beam, and collected by measuring the photocurrent from a Ni target.

Figure 2. Schematic layout of the U5 beamline.

Figure 3. U5 undulator spectra taken with a 1-mm pinhole nominally at the vertical center of the beam for three different horizontal positions: 3 mm to the right (top), at the beam center (center), and 3 mm to the left (bottom)

Figure 4. Schematic depicting the operation of the polarimeter for the measurement of horizontally (top) and vertically (bottom) polarized components of the undulator beam. The labels refer to: 1, undulator; 2, pinhole used upstream of the polarimeter; 3 multilayer Bragg-reflectors mounted at 45° with respect to the incident beam; 4 photodiode detector. (Note that items 3 and 4 always rotate together, thus they always remain in the same position relative to each other.)

Figure 5. Left scale shows an on-axis spectrum of the U5 undulator. The right scale shows the measured reflectivity of two of the multilayer Bragg-reflectors used for the polarization measurements. Note that each multilayer selects a different harmonic (the third and fourth).

Figure 6. Typical data (open circles) from polarization measurements as the polarizer/detector assembly rotates from -90° to 90°. The solid line is the best fit to a $\cos^2(\theta)$ angular dependence of the measured intensity.

Figure 7. Measured polarization as a function of angle for polarimeter located on the photon-beam center (boxes), and for the polarimeter located 3 mm below the beam center. Note that the lines serve only as a guide to the eye.

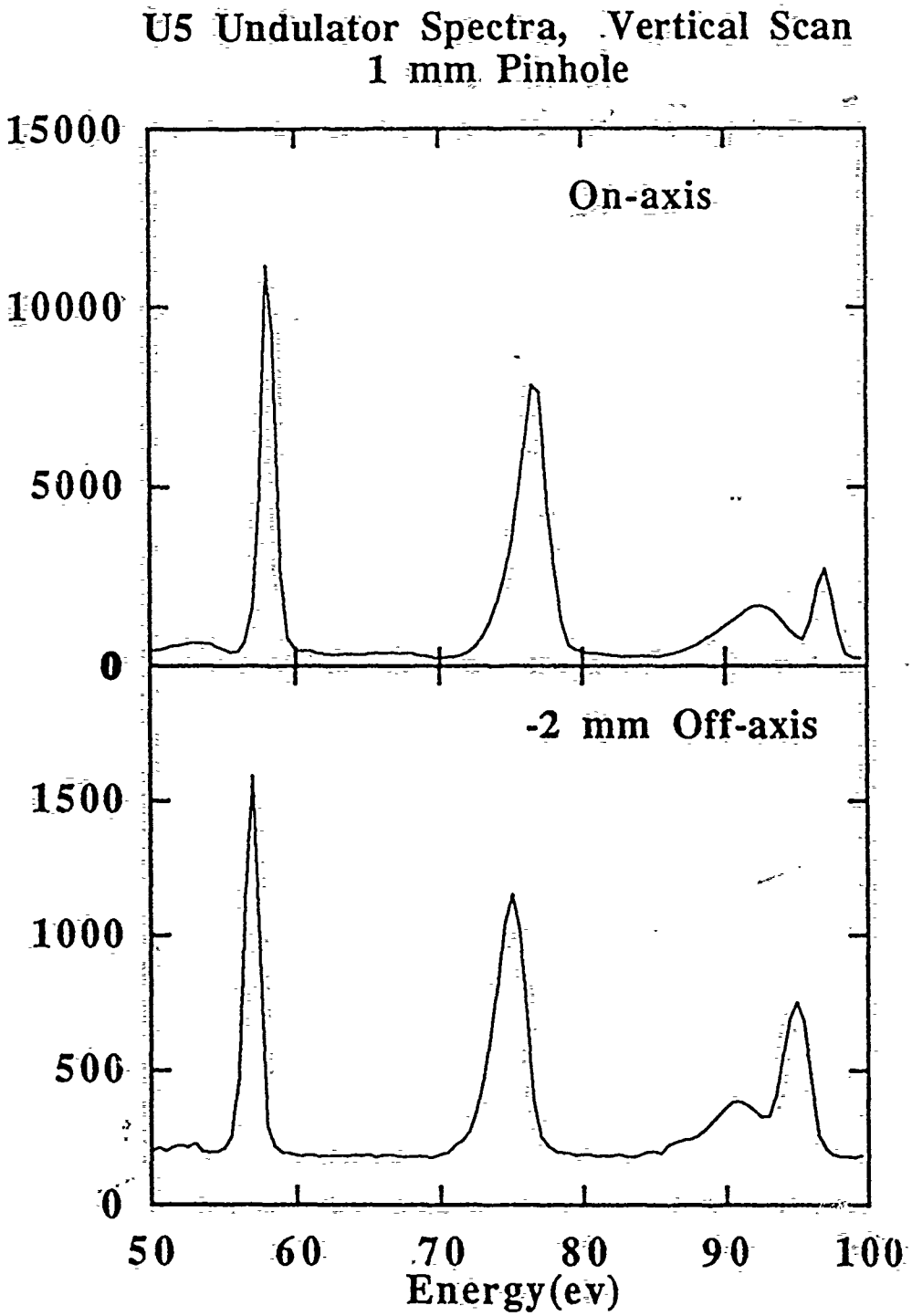
U5 Undulator Spectra, Vertical Scan
1 mm Pinhole
15000
10000
5000
0
On-axis
-2 mm Off-axis
1500
1000
500
0
50
60
70
80
90
100
Energy(ev)

Appendix I: Fig. 2

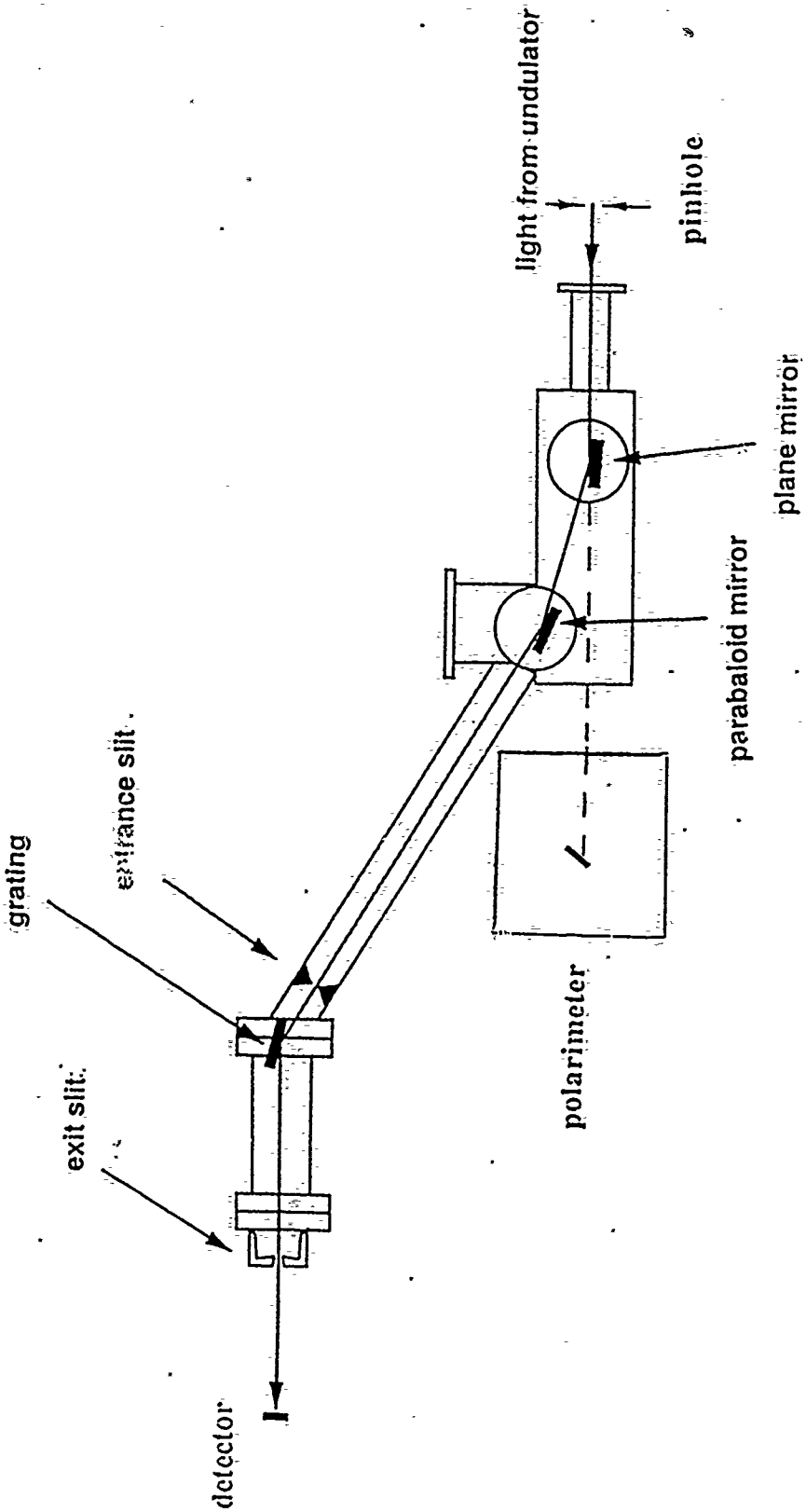

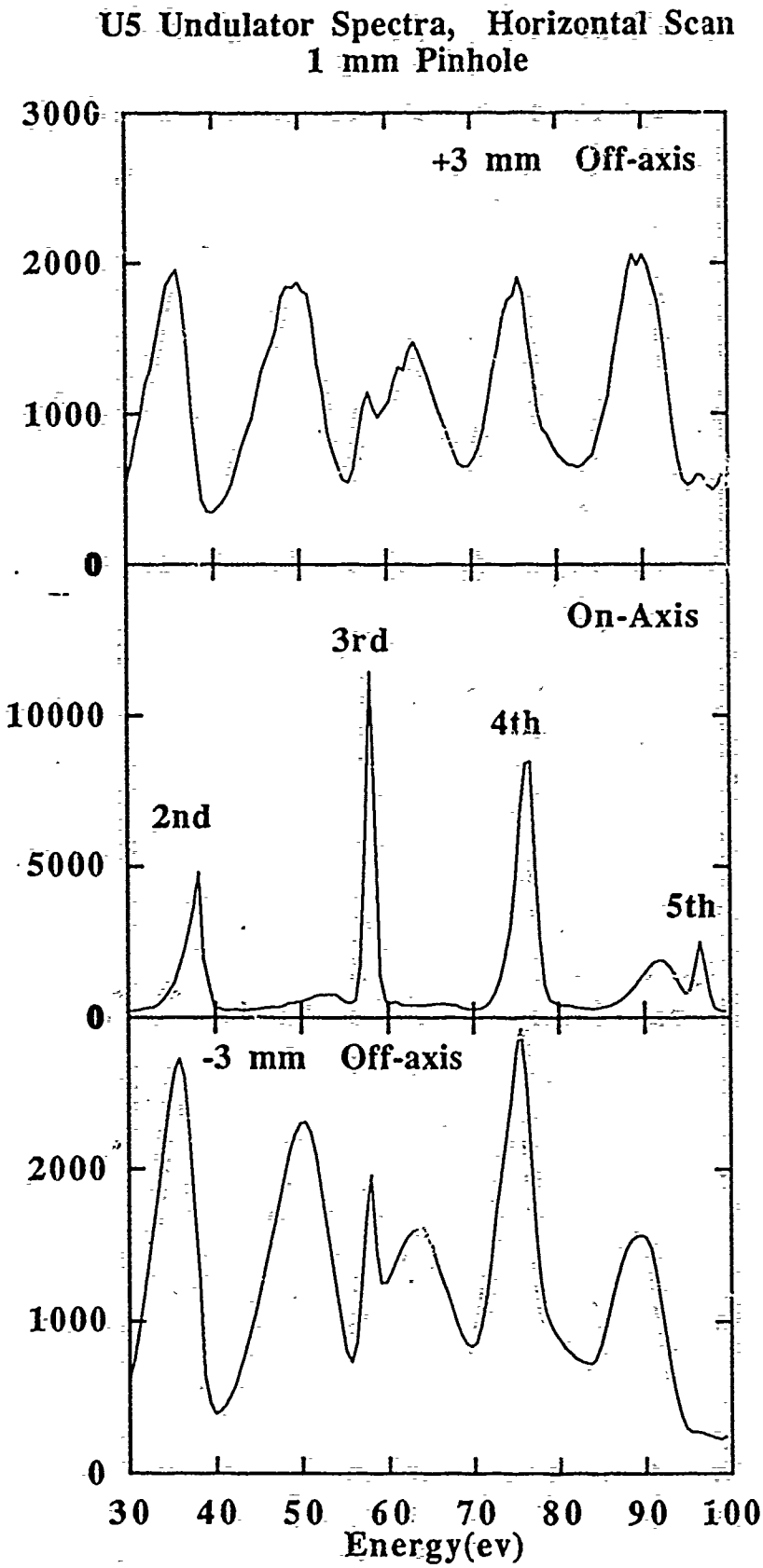
U5 Undulator Spectra, Horizontal Scan
1 mm Pinhole
+3 mm Off-axis
On-Axis
3rd
4th
2nd
5th
-3 mm Off-axis
3000
2000
1000
0
10000
5000
0
2000
1000
0
30 40 50 60 70 80 90 100
Energy(ev)

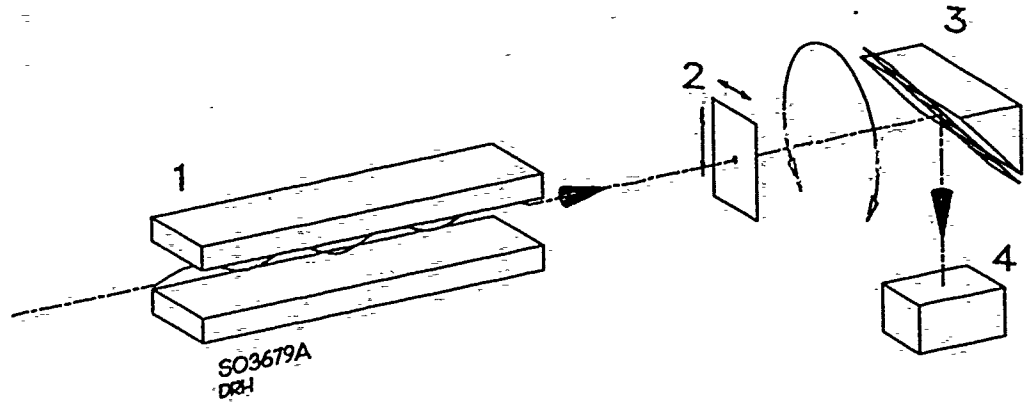
1
2
3
4
SO3679A
DRH

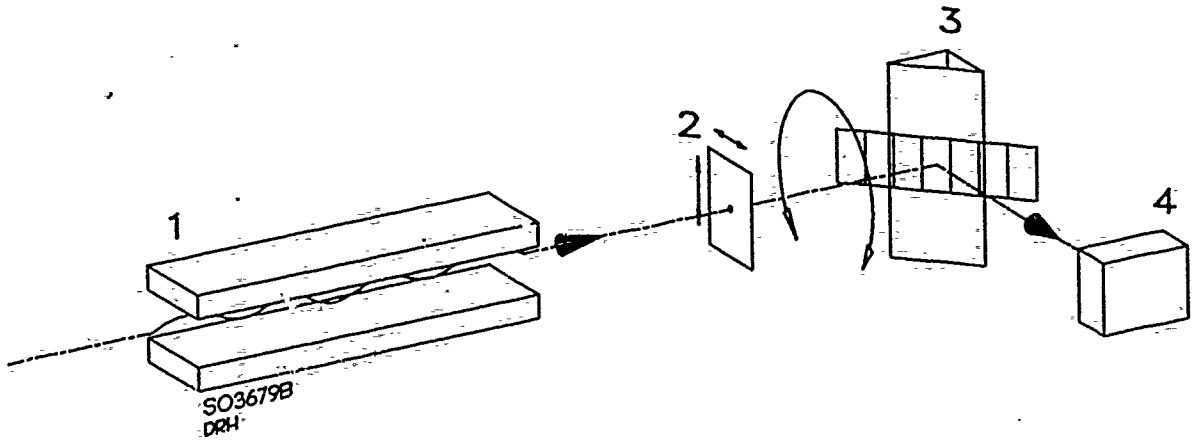
1
2
3
4
SO3679B
DRH

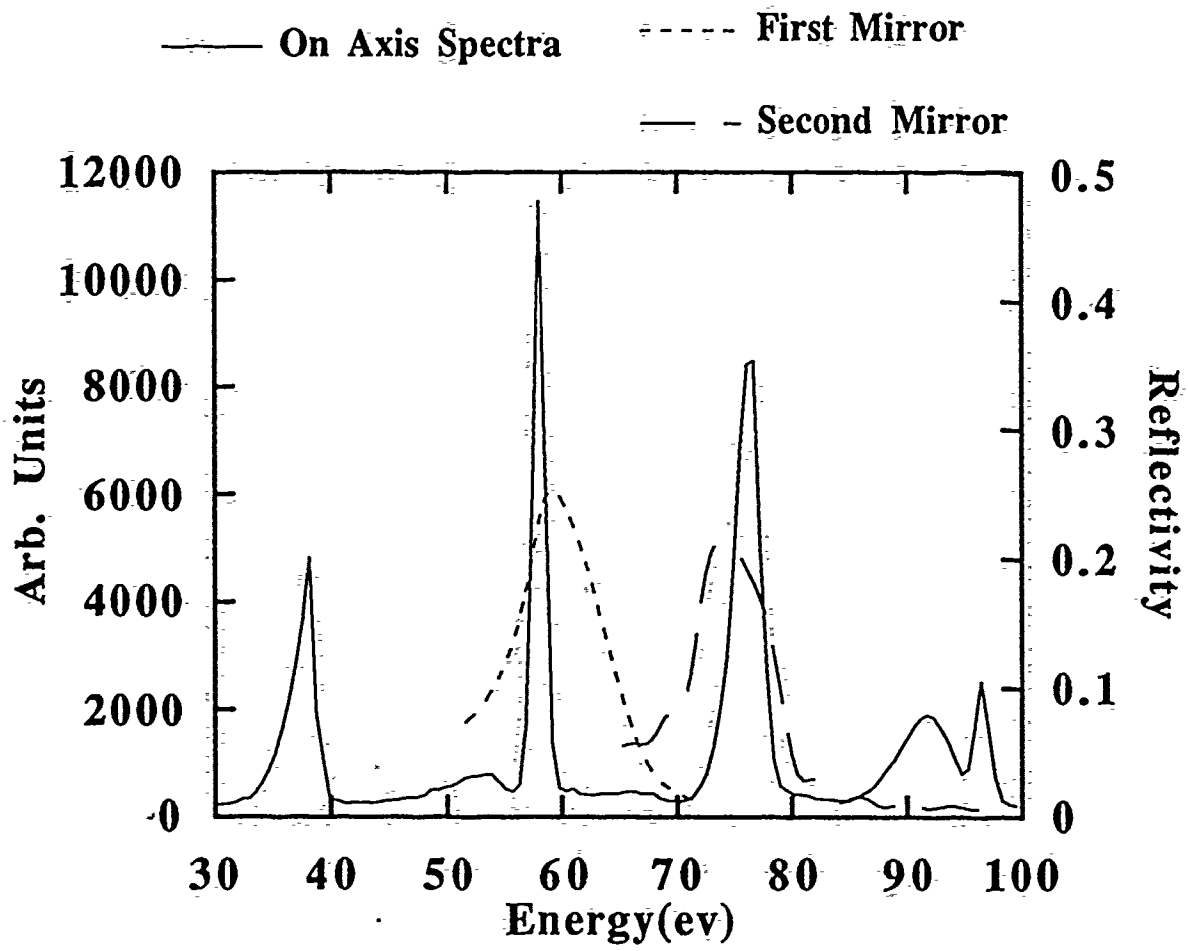
On Axis Spectra
First Mirror
Second Mirror
12000
10000
8000
6000
4000
2000
0
Arb. Units
0.5
0.4
0.3
0.2
0.1
0
Reflectivity
30
40
50
60
70
80
90
100
Energy(ev)

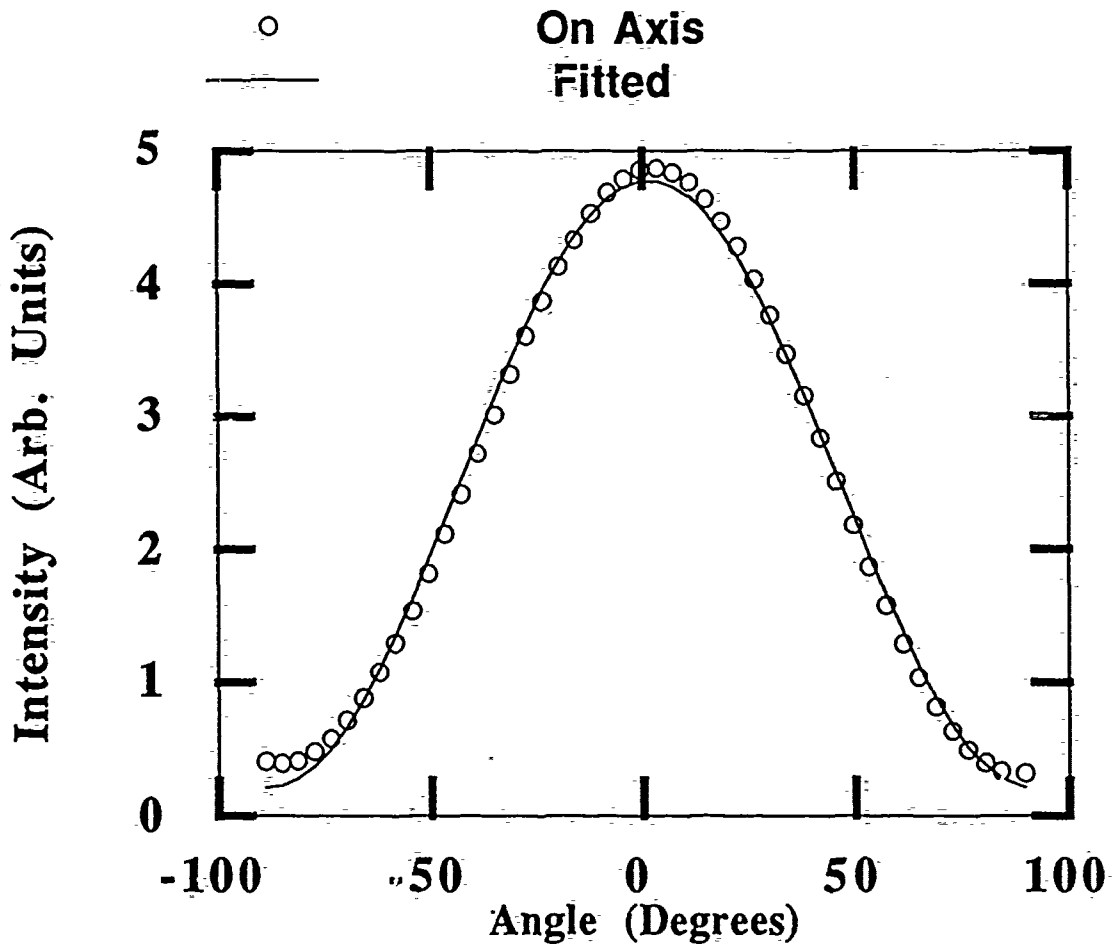
On Axis
Fitted
Intensity (Arb. Units)
0
1
2
3
4
5
-100
-50
0
50
100
Angle (Degrees)

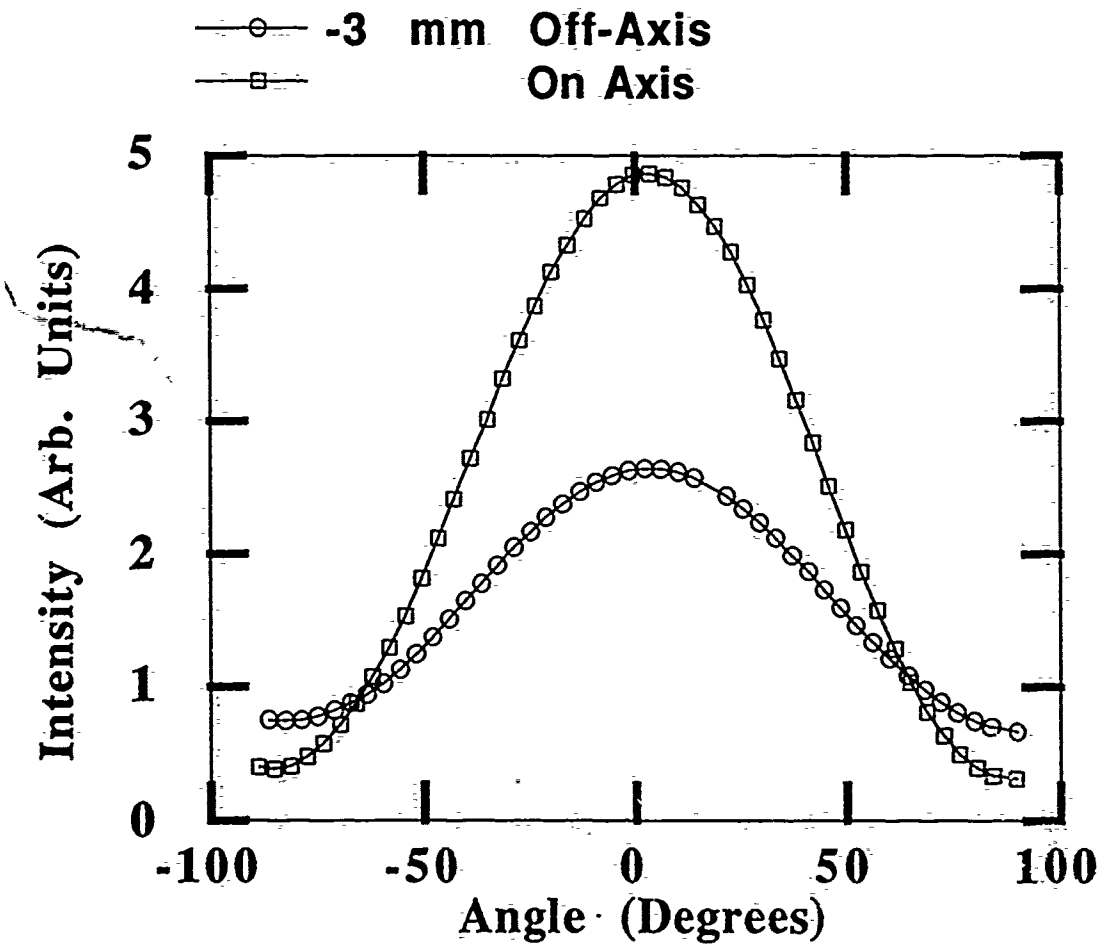
-3 mm Off-Axis
On Axis
Intensity (Arb. Units)
0
1
2
3
4
5
-100
-50
0
50
100
Angle (Degrees)

Comment on "Direct Observation of Spin-split Electronic States of Pd at the Pd(111)/Fe(110) Interface"

Y. Chang, N. B. Brookes, P. D. Johnson

Physics Department, Brookhaven National Laboratory, Upton, New York 11973

S. D. Bader

Materials Science Division, Argonne National Laboratory, Argonne, IL 60439

Comment on "Direct Observation of Spin-split Electronic States of Pd at the Pd(111)/Fe(110) Interface"

In a recent letter, Weber *et al.* [1] reported the observation of states localized within the interface formed between one atomic layer of Pd and an Fe(110) substrate. By examining the spin polarization, the authors concluded that the states represent an exchange-split pair whose relative binding energy is reversed with respect to that of the substrate bands. The authors noted that this observation is surprising, especially in view of the fact that their own magnetometry measurements indicate a net positive induced Pd moment at the Pd/Fe interface, i.e. a ferromagnetic alignment. They also suggest that a calculation by Huang *et al.* [2] of a pseudomorphic Pd monolayer on a three-layer Fe(001) slab agrees qualitatively with their observation, because the calculation indicates a positive moment induced on the Pd as well as an apparent inverted exchange splitting in the spin-resolved density of states. We note, however, that Huang *et al.* [2] showed only the spin components of the total density of states, rather than a detailed band structure from which spin exchange splittings for different bands can be obtained.

In any spin-resolved photoemission experiment, the identification of exchange split components requires the demonstration that the states have different spin character and, further, have the same symmetry. The latter observation is made by varying the effective polarization of the incident light and employing symmetry dependent selection rules. It should be noted, however, that the identification of valence states with the same symmetry but different spin character cannot necessarily be used to determine the alignment

or even the existence of a moment. Such information can only be extracted by examining the total spin-dependent density of states.

We have recently studied the interface formed by depositing Pd on an Fe(001) surface using spin-resolved photoemission. LEED studies of this system indicate a p(1x1) overlayer. The detailed results will be presented elsewhere. Here we would like to demonstrate that the spin-resolved interface states Weber *et al.* [1] observed are probably not exchange split components. Figure 1 shows our spin and angle-resolved photoemission spectra taken at normal emission from 1 atomic layer of Pd on Fe(001), with either s- or p-polarized light with photon energy 58 eV. These spectra are obtained with linearly polarized light at an angle of incidence of 35^0 and 70^0 respectively. We observe a number of spin-resolved peaks including one majority peak at 1.5 eV binding energy and one minority peak at 1.7 eV binding energy. The latter peak is clearly associated with the overlayer, there being no structure at this binding energy on the clean surface. Coverage dependent spectra show the two peaks in fig. 1 to be localized at the interface. Spectra with 19.5 eV photons (not shown here) show the same two peaks with line shapes very similar to those of Weber *et al.* [1]. Thus, the Pd/Fe(001) interface again appears to show an inverted exchange splitting. Examination of fig. 1, however, shows that the two peaks show a different sensitivity to the incident light polarization and hence have a different symmetry. Certainly for this interface then the peaks do not represent an exchange split pair. We suggest that a similar result may be found for the Pd/Fe(1-10) interface if the symmetry of the states is examined. This would then remove any discrepancy between the measured electronic structure and the magnetometry measurements.

This work was supported in part by the U.S. Department of Energy under Contract Nos. DE-AC02-76CH00016 and W-31-109-ENG-38 and the National Science Foundation under Contract No. DMR-86-03304.

References

1. W. Weber, D. A. Wesner, G. Guntherodt, and U. Linke, Phys. Rev. Lett. **66**, 942 (1991).

2. H. Huang, J. Hermanson, J. G. Gay, R. Richter, and J. R. Smith, Surf. Sci. **172**, 363 (1986).

Figure Caption

Figure 1.

Spin and angle-resolved photoemission valence band spectra of 1 monolayer of Pd on Fe(001), taken at normal emission with 58 eV photons. The upper panel shows the spectrum taken with mainly s-polarized light, and the lower panel shows the spectrum with more p-polarized light. The arrows identify the features at 1.5 and 1.7 eV binding energy, which are not spin-plit pairs because of their different polarization dependences.

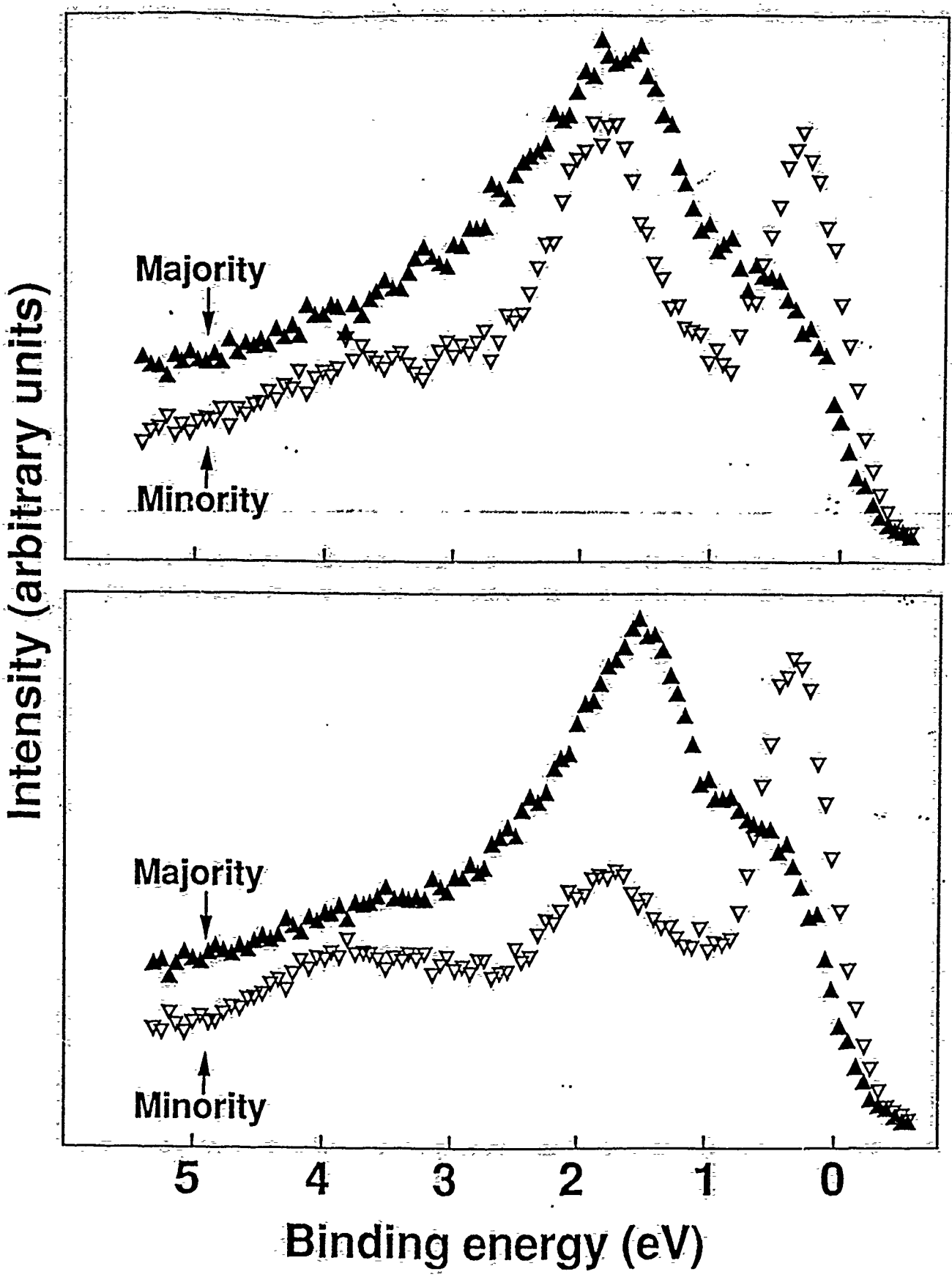
Majority
Minority
Majority
Minority
Intensity (arbitrary units)
5
4
3
2
1
0
Binding energy (eV)

VOLUME 67, NUMBER 3 PHYSICAL REVIEW LETTERS 15 JULY 1991

Magnetic Interface States and Finite-Size Effects

N. B. Brookes, Y. Chang, and P. D. Johnson

Physics Department, Brookhaven National Laboratory, Upton, New York 11973

(Received 13 March 1991)

Studies of the formation of a nonmagnetic/magnetic silver/iron interface by spin-polarized photoemission identify magnetic interface states showing discrete binding energies dependent on the number of atomic layers in the overlayer. The results for one layer of silver on iron are in good agreement with a full-potential linearized-augmented-plane-wave calculation and tight-binding modeling allows us to reproduce qualitatively the layer-dependent binding energies for one, two, and three layers of silver on iron. The interface states appear to be related to a minority surface resonance on the iron surface.

PACS numbers: 79.60.Cn, 75.70.Cn

In recent years there has been considerable interest in the properties of magnetic surfaces [1], thin films [2], and multilayers [3]. Much of the experimental work has been oriented towards understanding two-dimensional magnetic phenomena; testing predictions of enhanced magnetic moments at surfaces and in thin films [4], and understanding the properties that determine anisotropy in these films [5]. The technological drive for such experiments lies in the possibility of tailoring new materials for the recording and device industries. In early work [6] the magnetic thin films were covered with a nonmagnetic protective coating such as silver before making the magnetic measurements. Initial disagreement between experiments and theory, particularly in the hyperfine splittings, was resolved with calculations [7] showing that significant changes in the electronic structure occur at the interface. Such interfacial properties may also be important when many repeat units of these thin-film systems (i.e., multilayers) are grown. Indeed, recent theoretical work [8] has emphasized the interfacial properties as a possible explanation of the magnetic coupling in certain transition-metal multilayer systems, examples of which include iron/chromium [9,10] and iron/copper [11,12] superlattices. In such systems it is possible to achieve either ferromagnetic or antiferromagnetic coupling of adjacent ferromagnetic iron layers depending on the thickness of the intervening layer. The model is similar to a picture [13] which has already been used to describe the magnetic properties of rare-earth compounds and superlattices, where the Coulomb exchange interaction is of paramount importance. In the case of transition metals on the other hand, the hybridization interaction at the interface is assumed to be the dominant effect. The related giant magnetoresistance properties [10] of the Fe/Cr superlattices and the large enhancement of the Kerr rotation [12] in the Fe/Cu multilayers make these systems particularly interesting.

In this Letter we describe spin-polarized photoemission experiments that directly probe the electronic states at a magnetic/nonmagnetic metal interface formed by depositing silver on an iron substrate. We are able to demonstrate that the binding energy of the interface states are strongly layer dependent—as the silver thickness increases these states move up to and probably through the Fermi level. Spin-polarization analysis of the photoemitted electrons shows that these localized interface states are magnetic. *Thus both the electronic and the magnetic properties of the interface may be modified by the presence of the nonmagnetic thin film.* Such effects may well need to be taken into account when the properties of overlayers and multilayers are being considered. By comparing our experiments with the results of tight-binding calculations we are able to show that the presence of the silver overlayers leads to the localization of a previously identified iron surface resonance [14] into the region of the interface. Similar observations have already been made for the Nb/Pd interface [15] where a Nb surface resonance again localizes in the interface and for the Pd/Fe interface [16] where a spin-split interface state in the Pd 4*d* bands has been reported. However, unlike in those studies, the present experiment finds a discrete new binding energy for the interface state as each layer of silver is deposited. These observations are qualitatively reproduced in our tight-binding modeling.

The spin-polarized photoemission experiments reported here were carried out on an apparatus which will be described in detail elsewhere [17]. Briefly, spin detection is achieved with a compact low-energy spin detector [18] and uses light provided by the U5 VUV undulator at the National Synchrotron Light Source. The angular resolution of the hemispherical analyzer was $\pm 1.5°$ and the combined photon and analyzer energy resolution was 0.35 eV. The Fe(001) crystal was manufactured in the form of a picture frame with each leg along a ⟨100⟩ direction and magnetized using a coil wound around one leg. The crystal was cleaned by repeated argon-ion bombardment and annealing cycles. The surface contamination level was monitored initially using Auger electron spectroscopy and in the final stages using photoelectron spectroscopy. The surface crystallographic order was examined with low-energy electron diffraction (LEED).

The silver films were evaporated at room temperature and at a rate of approximately 0.25 monolayer (ML) per minute. The iron and silver Auger ratios were measured as an estimate of the coverage and the evaporations were monitored using a quadrupole mass spectrometer. LEED measurements showed a good sharp $p(1\times1)$ pattern at all coverages up to approximately 3 ML, after which the patterns became less sharp. As a result, in the following discussion we restrict our observations to the first three

monolayers.

The tight-binding calculations [19] were carried out for thirteen layers of iron and with one to four layers of silver (a total of 21 layers for the thickest films). A two-center nonorthogonal basis set was used, the parameters being taken from Papaconstantopoulos [20]. The silver-iron interaction parameters were taken as the mean of the iron and silver parameters [21] and where required the scaling scheme of Andersen and co-workers [20–22] was used. The on-site silver energies were also adjusted to align the silver and iron Fermi levels. The iron and silver lattice constants were taken as the bulk values and for the interfacial separation the mean of the iron and silver interlayer spacings was used following Fu and Freeman [23]. The calculations for a thirteen-layer iron film and the same film with a silver monolayer were compared with the results of a full-potential linearized-augmented-plane-wave (FLAPW) calculation [7,24] and found to be in good agreement. No attempt was made to adjust the parameters so as to fit the experimental observations as the principle aim was to examine trends.

Figure 1 shows the evolution of the spin-integrated angle-resolved photoemission spectra at normal emission

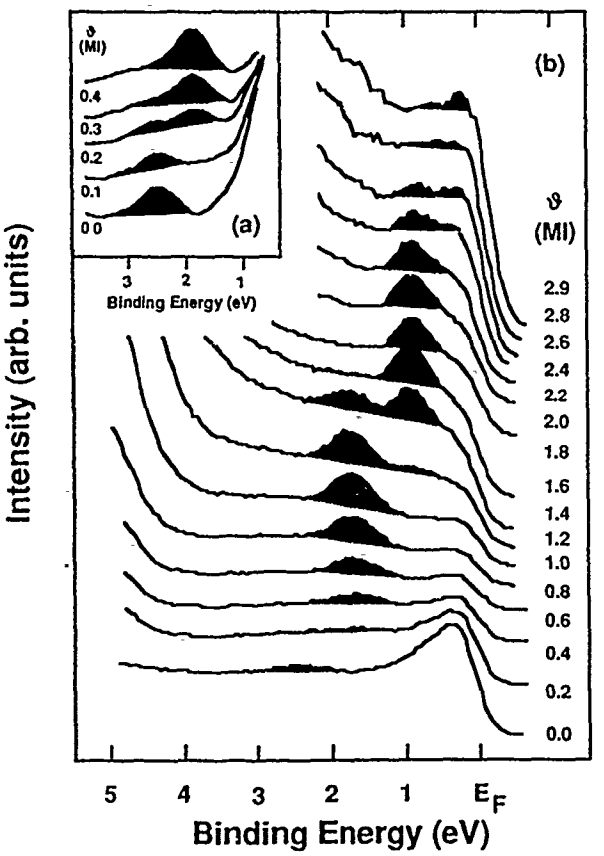

FIG. 1. Normal-emission angle-resolved photoemission spectra at a photon energy ($h\nu$) of 52 eV and p-polarized light ($\varphi_i = -70°$), showing the evolution of the spectra with increasing silver overlayer thickness (ϑ) in monolayers (ML) for (a) the low coverage regime 0.0–0.4 ML and (b) coverages up to ~3 ML.

and 52-eV photon energy with increasing silver coverage. (For clarity the number of spectra shown has been limited, data were collected for every 0.1 ML of silver.) The region within the first 4 eV of the Fermi level includes the iron d bands and the silver s-p bands. For the bulk materials the photoemission spectra are characterized by a peaked structure near the Fermi level for iron and for silver by structureless intensity stretching from the Fermi level to the start of the silver d bands at ~4-eV binding energy. The feature at 2.4-eV binding energy on the clean Fe(001) surface [Fig. 1(a)] has previously been identified as a minority-spin surface resonance [14]. As the silver coverage is increased this feature attenuates and is no longer observable at ~0.4-ML silver coverage. However, after only ~0.2-ML silver deposition a new feature at 1.7-eV binding energy is seen to coexist with the surface resonance. This new feature continues to increase in magnitude, maximizing at approximately 1-ML coverage [Fig. 1(b)]. As the second monolayer starts to form, the peak decreases in intensity and from 1.2 ML another feature at 1-eV binding energy is observed. The 1.7-eV peak, which we associate with a single monolayer film, continues to decrease in intensity. The peak at 1 eV we correlate with the 2-ML film since it peaks in intensity at 2-ML coverage and then decreases in intensity as the third layer is deposited. Although the features in successive layers are getting weaker, a new feature at approximately 0.3-eV binding energy is still seen to grow in and we associate this with the three-layer silver film. We assume that for higher coverages the peak would move through the Fermi level.

It is evident that for each silver/iron overlayer system, 1, 2, or 3 ML, there is a distinct electronic state associated with it. The attenuation of the intensity of the peaks as a function of coverage is consistent with their being states at the iron/silver interface, which is continuously buried. Since all these states have the same symmetry (as determined by their dependence on the polarization of the incident light) and the minority-spin surface resonance is attenuated [see Fig. 1(a)] on depositing silver rather than extinguished as in the case of oxygen absorption, we look for a common origin by investigating their spin character. Figure 2 shows that a dip in the spin polarization corresponding to the position of each of the overlayer states is observed; this is as a result of all the states being of minority character. The corresponding majority states are broader, weaker, and not so easily resolved from the substrate features. Consequently, in the following we will concentrate on the minority states. With increasing silver deposition the overall level of spin polarization is diminished and in a manner which is consistent with covering a magnetic substrate with a nonmagnetic overlayer. Further, the observation that the states are magnetic lends support to the proposal that they are located in the interface rather than in the silver layer.

It should be noted that the iron d bands (Fig. 1) ap-

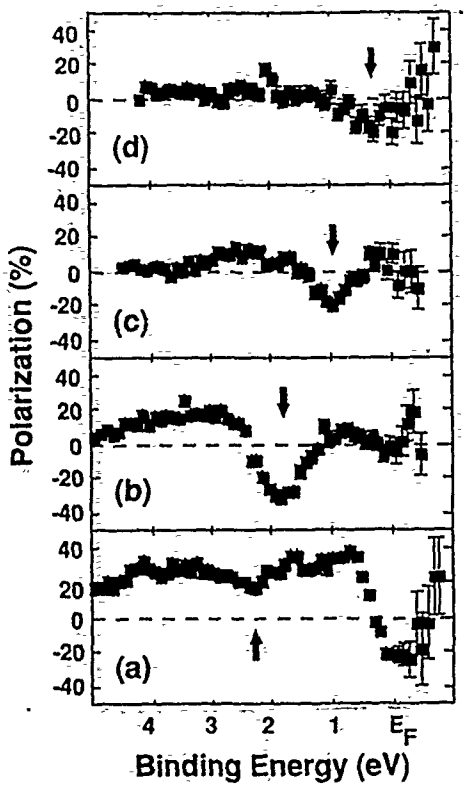

FIG. 2. Spin-polarization spectra taken at normal emission, $h\nu = 52$ eV and $\varphi_i = 70°$ for (a) clean Fe(001) and with silver overlayers, (b) 1 ML, (c) 2 ML, and (d) 3 ML thick. The arrows mark the positions of the peaks in the photoemission spectra shown in Fig. 1 for each coverage.

pear to attenuate much more rapidly than one would expect for small silver coverages. This is largely due to the substantial surface contribution to the iron spectrum under these experimental conditions. For instance, a 0.1-L oxygen dose (1 L = 10^{-6} Torr s) decreases the iron spectral intensity by ~50%. At photon energies (e.g., $h\nu$ = 37 eV) where the spectra are less dominated by surface features, the d bands are more prominent and the interfacial features are relatively weaker.

Several earlier experimental studies of thin-film growth have identified layer-dependent states in both silver [25] and alkali-metal overlayers [26]. The results of these experiments have been interpreted in terms of a phase model analogous to that used in the discussion of surface-state formation [27]. Thus the analysis involves a phase shift of $2kd$ within the thin film, or potential well, where d is the thickness of the film and k is the free electron wave number representing the state within the well. Although not included in the phase model the periodic structure within the well is reflected in the thicker silver films in that eventually the allowed states map the band states of the overlayer [25]. In the present study the films are still within the ultrathin regime where it is less obvious that the "bulk" band structure of the overlayer will play a role. However, it may be anticipated that the periodic structure of the film will still result in quantization effects dependent on the film thickness [28]. This could then lead to states moving to or away from the Fermi level depending on the individual case. The initial iron surface resonance from which these states are derived involves d states as well as s and p states and does not therefore lend itself to a rigorous treatment within the phase analysis, which was originally demonstrated for s-p–derived states [27]. We therefore chose to compare our results with thin-film calculations and use a tight-binding description to discuss the layer dependence of the interface states.

The interfacial nature of the observed state for 1 ML of silver on iron can be confirmed by comparison with a FLAPW thin-film calculation [7,24]. A minority interface state (more than 67% of the character being in the silver and iron interfacial layers) is found; it has the correct symmetry and is at a binding energy of ~1.6 eV, which correlates well with the observed feature at ~1.7-eV binding energy (Fig. 1). The FLAPW calculations for the uncoated iron surface find a minority surface resonance [14] localized in the outer two iron layers (> 55%); the Ag/Fe interface state can be thought of as arising from a hybridization of the iron surface resonance, which is of s-p_z-d_{z^2} character, with the silver bands of the same symmetry—the s-p band at a similar binding energy and the silver $4d$ bands at deeper binding energies. For the thicker silver coverages no first-principles calculation is available. However, our tight-binding results for one layer of silver on iron show qualitatively similar results to the FLAPW calculations; we find a state localized at the interface and at ~2-eV binding energy. The tight-binding method allows us to extend our calculations to thicker silver films without carrying out prohibitively large first-principles calculations. The results for two layers of silver show an interfacial feature closer to the Fermi level than for 1 ML, as is observed experimentally; however, the calculated shift of ~0.3 eV is less than that observed (~0.7 eV). The difference probably reflects the increased importance of the s-p band in the thicker films and the poor treatment of these states in the tight-binding model. The two-layer state, although predominantly centered at the interface, is slightly less localized than for one layer, its weight extending into the outer (second) silver layer. This can be seen in Fig. 3 which shows the layer-resolved charge density for the interface states as determined from the tight-binding calculations. The calculations for three and four layers of silver show a similar trend, states with substantial weight at the interface are found and they successively move closer to the Fermi level. Beyond two layers significant intensity also develops in the outer silver layer (Fig. 3). This is most clearly observed for the four-layer film and reflects the formation of a silver surface band. The latter's orbital character is predominantly p_z and it appears to be related to the s-p_z surface resonance on silver which occurs approximately 1 eV above the Fermi level, as determined from a thirteen-layer silver tight-binding calculation [29] and from the application of the phase model [27].

In summary, both the experimental and theoretical

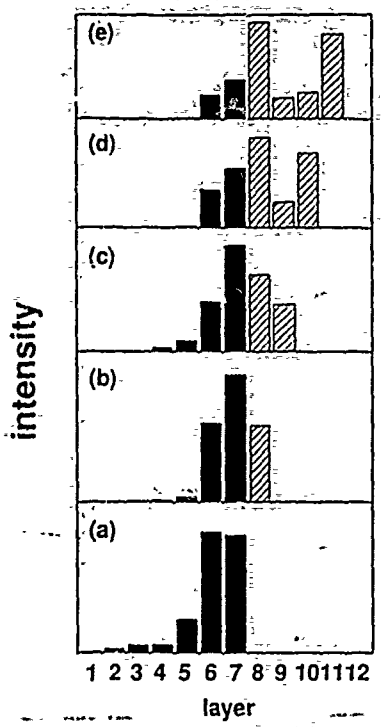

FIG. 3. The intensity per layer for (a) the minority surface resonance, and the minority interface states for (b) one layer, (c) two layers, (d) three layers, and (e) four layers of silver on iron as determined from the tight-binding modeling. The iron layers are shown in black and the silver is hatched. Layer 1 is the center of the slab and layer 7 is the outermost iron layer.

work are consistent with the conclusion that we have observed magnetic interface states. Their binding energy strongly depends on the thickness of the nonmagnetic overlayers and further they appear to be related to the surface properties of iron. The tight-binding modeling is qualitatively in agreement with the measurements, the movement of the interface states towards the Fermi level being reproduced. In addition, since there is appreciable intensity in the silver layers, for these minority-spin states, we can conclude that there are spin-dependent states on the silver sites. The observation that the interfacial electronic structure is related to the surface properties and that there are distinct size effects is of import to theoretical models which depend on the electronic structure at the interface.

We are indebted to Mike Weinert for many discussions concerning the tight-binding calculations and Andrew Clarke for help with the initial development of our layered scheme. This work was supported in part by the U.S. Department of Energy Contract No. DE-AC02-76CH00016 and National Science Foundation Materials Research Group Contract No. DMR-86-03304.

[1] A. J. Freeman, C. L. Fu, S. Ohnishi, and M. Weinert, in *Polarized Electrons in Surface Physics*, edited by R. Feder (World Scientific, Singapore, 1985), Chap. 1.

[2] *Magnetism in Ultrathin Films*, edited by D. Pescia, special issue of Appl. Phys. A **49** (1989).

[3] L. M. Falicov, D. T. Pierce, S. D. Bader, R. Gronsky, K. B. Hathaway, H. J. Hopster, D. N. Lambeth, S. S. P. Parkin, G. Prinz, M. Salamon, I. K. Schuller, and R. H. Victora, J. Mater. Res. **5**, 1299 (1990).

[4] For example, H. J. Elmers, G. Liu, and U. Gradmann, Phys. Rev. Lett. **63**, 566 (1989).

[5] B. T. Jonker, K.-H. Walker, E. Kisker, G. A. Prinz, and C. Carbone, Phys. Rev. Lett. **57**, 142 (1986); N. C. Koon, B. T. Jonker, F. A. Volkening, J. J. Krebs, and G. A. Prinz, Phys. Rev. Lett. **59**, 2463 (1987).

[6] J. Tyson, A. H. Owens, J. C. Walker, and G. Bayreuther, J. Appl. Phys. **52**, 2487 (1981).

[7] S. Ohnishi, M. Weinert, and A. J. Freeman, Phys. Rev. B **30**, 36 (1984).

[8] Y. Wang, P. M. Levy, and J. L. Fry, Phys. Rev. Lett. **65**, 2732 (1990).

[9] P. Grunberg, R. Schreiber, Y. Pang, M. B. Brodsky, and H. Sowers, Phys. Rev. Lett. **57**, 2442 (1986).

[10] M. N. Baibich, J. M. Broto, A. Fert, F. Nguyen Van Dau, and F. Petroff, P. Eitenne, G. Creuzet, A. Friederich, and J. Chazelas, Phys. Rev. Lett. **61**, 2472 (1988).

[11] B. Heinrich, Z. Celinski, J. F. Cochran, W. B. Muir, J. Rudd, Q. M. Zhong, A. S. Arrott, K. Myrtle, and J. Kirschner, Phys. Rev. Lett. **64**, 673 (1990).

[12] W. R. Bennett, W. Schwarzacher, and W. F. Egelhoff, Jr., Phys. Rev. Lett. **65**, 3169 (1990).

[13] Y. Yafet, J. Appl. Phys. **61**, 4058 (1987).

[14] N. B. Brookes, A. Clarke, P. D. Johnson, and M. Weinert, Phys. Rev. B **41**, 2643 (1990).

[15] X. Pan, P. D. Johnson, M. Weinert, R. E. Watson, J. W. Davenport, G. W. Fernando, and S. L. Hulbert, Phys. Rev. B **38**, 7850 (1988).

[16] W. Weber, D. A. Wesner, G. Guntherodt, and U. Linke, Phys. Rev. Lett. **66**, 942 (1991).

[17] P. D. Johnson, S. L. Hulbert, R. Klaffky, N. B. Brookes, A. Clarke, B. Sinković, and M. Kelly (to be published).

[18] J. Unguris, D. T. Pierce, and R. J. Celotta, Rev. Sci. Instrum. **57**, 1314 (1986).

[19] J. C. Slater and G. F. Koster, Phys. Rev. **94**, 1498 (1954).

[20] D. A. Papaconstantopoulos, *Handbook of the Band Structure of Elemental Solids* (Plenum, New York, 1986).

[21] J. D. Shore and D. A. Papaconstantopoulos, Phys. Rev. B **35**, 1122 (1987).

[22] O. K. Andersen and O. Jepsen, Physica (Amsterdam) **91B**, 317 (1977); O. K. Andersen, W. Klose, and H. Nohl, Phys. Rev. B **17**, 1209 (1978).

[23] C. L. Fu and A. J. Freeman, Phys. Rev. B **33**, 1611 (1986).

[24] M. Weinert (private communication).

[25] A. L. Wachs, A. P. Shapiro, T. C. Hsieh, and T.-C. Chiang, Phys. Rev. B **33**, 1460 (1986); T. Miller, A. Samsavar, G. E. Franklin, and T.-C. Chiang, Phys. Rev. Lett. **61**, 1404 (1988).

[26] S. Å. Lindgren and L. Walldén, Phys. Rev. Lett. **59**, 3003 (1987); **61**, 2894 (1988).

[27] N. V. Smith, Rep. Prog. Phys. **51**, 1227 (1988).

[28] P. D. Loly and J. B. Pendry, J. Phys. C **16**, 423 (1983).

[29] N. B. Brookes, Y. Chang, and P. D. Johnson (unpublished).

SPIN POLARIZED PHOTOEMISSION STUDIES OF SURFACES AND THIN FILMS

PETER D. JOHNSON, N. BROOKES and Y. CHANG
Physics Dept., Brookhaven National Laboratory, Upton NY 11790.

ABSTRACT

Spin polarized photoemission is used to study the magnetic states associated with the clean iron (001) surface. These studies reveal evidence for a minority spin surface state in agreement with first principles calculation. Studies of the same surface with silver and chromium epitaxial overlayers reveal evidence for interface states derived from the states found on the clean surface. In the case of the silver overlayer the binding energy of this state is found to be dependent on the layer by layer thickness of the overlayer. With chromium overlayers the binding energy for the same interface state does not show the same thickness dependence. However a second interface state is observed immediately below the Fermi level.

INTRODUCTION.

In recent years there has been a marked increase in research activity in the general area of surface magnetism including the magnetic properties of surfaces [1], thin films [2] and multilayers [3]. Much of the work in the latter area has been motivated by the observation that in certain transition metal multilayers, an example being the Fe/Cr system, alternate ferromagnetic layers may be made to align either parallel or anti-parallel depending on the thickness of the intervening layer [4]. Further in the same systems enhanced magnetoresistance effects have also been observed [5]. The period of the oscillations is not easily explained by a simple RKKy type interaction and hence several explanations have been proposed for the phenomena. One model proposes that the oscillations in the coupling reflect size quantization of hole states trapped in the nonmagnetic medium between the layers [6]. An alternative model relies on coupling of states localized in the interface through hybridization with conduction electrons in the intervening layer [7]. Clearly a better knowledge of the spin dependent electronic structure of these materials will be of benefit in any attempt to elucidate the correct mechanism.

Spin polarized photoemission with the capability of identifying two and three dimensional electronic states represents an excellent tool for such studies. The technique is however limited by the mean free path or escape depth of the photoelectrons. This limitation makes it more difficult to study directly the multilayer systems. However the interfaces may be studied by growing them in situ using molecular beam epitaxial growth methods.

In this paper we describe spin polarized photoemission experiments, which examine the magnetic structure of the clean iron (001) surface and modifications to this structure through the growth of thin film overlayers of silver and chromium. We are able to show that, as predicted, magnetic surface states or resonances exist at the iron (001) surface. With the deposition of epitaxial overlayers these states appear to become more localized in the interface region.

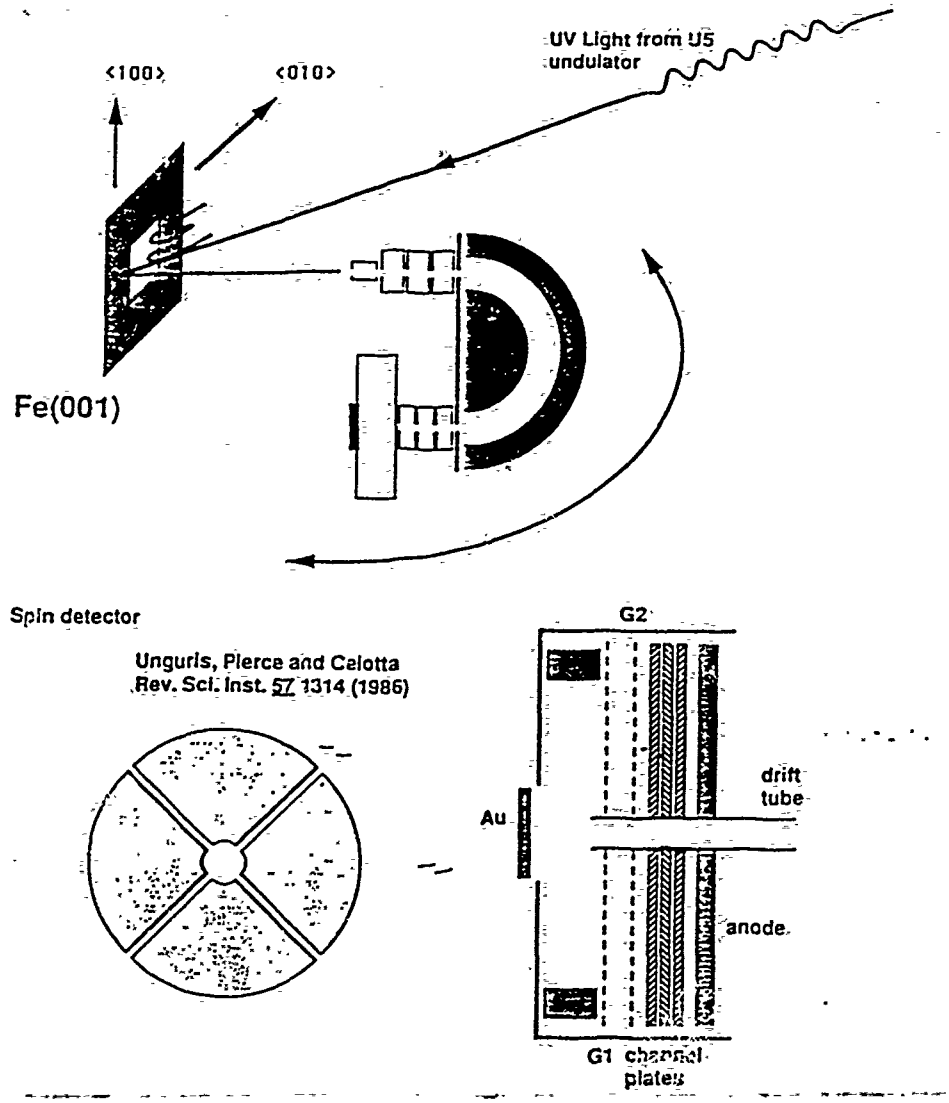

Fig.1 Schematic diagram of the apparatus used for spin polarized photoemission. Upper level: light from the U5 undulator excites photoelectrons which are detected by a hemispherical electron spectrometer. This analyser is coupled via an exit lens to a spin detector. Lower level: arrangement of the spin detector of the type described by Unguris et al. (ref. 9). G1 and G2 represent energy selecting retard grids. Four discrete anodes collect the scattered electrons as indicated at the lower left side.

As the thin film grows the interface states are found to be continuously sensitive to the changing boundary conditions, particularly in the case of the iron-silver interface where each newly deposited silver layer results in a discrete new binding energy for the state. For the chromium-iron interface two new states are observed with one state sitting immediately below the Fermi level.

EXPERIMENTAL.

The experiments described in this paper were carried out on a spin polarized photoemission facility [8] established on the U5 UV undulator at the

NSLS. Shown schematically fig. 1, a commercial hemispherical electron spectrometer, equipped with a low energy spin detector of the type described by Unguris et al. [9] is mounted on a goniometer allowing the full flexibility of angle resolved measurements. Measurement of a spin dependent asymetry in the scattering of low energy, 150 eV, electrons from a polycrystalline gold target is used to determine the polarization of the photoemitted electrons. The low efficiency or figure of merit of the spin detector, 10-4, is more than compensated for by the high photon flux available from the undulator. The experimental chamber is also equipped with Low Energy Electron Diffraction (LEED) and Auger Electron Spectroscopy (AES) for surface characterization.

Fcc silver and bcc chromium have a nearly perfect lattice match for growth on a bcc iron (001) substrate, the appropriate interatomic spacings being 2.88, 2.86 and 2.87 Å respectively. The metal overlayers were produced from electron beam evaporators with deposition rates monitored by both AES and by evaporating directly into a quadrupole mass spectrometer. Silver films were deposited on an iron (001) substrate at room temperature but in order to study the same interface it was found to be necessary to evaporate iron films on a silver

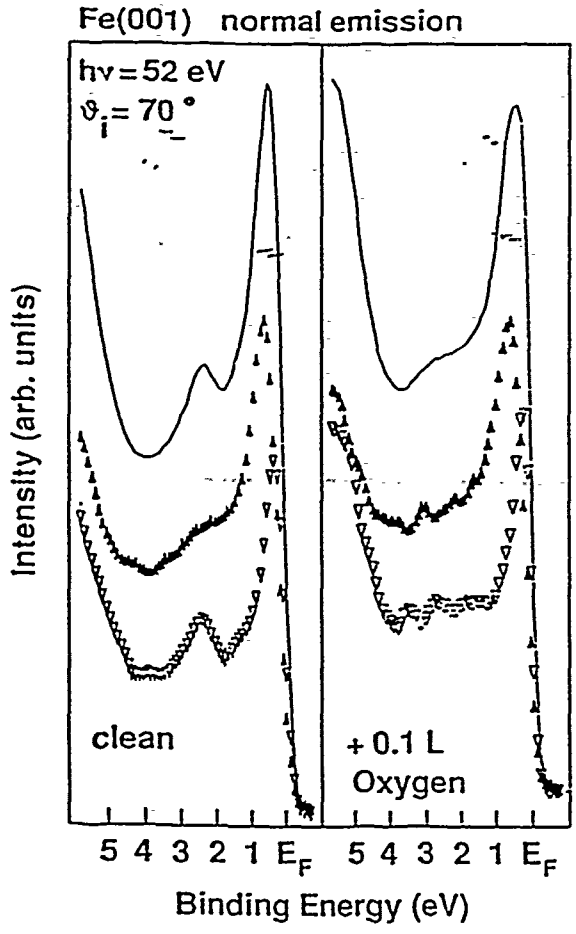

Fig.2. Photoemission spectra recorded for emission along the surface normal from the clean surface and the same surface following exposure to 0.1L of oxygen. Solid and open triangles indicate the spin resolved majority and minority spin spectra respectively. The incident photon energy was 52 eV with an angle of incidence corresponding to p polarized light.

(001) substrate at a lower temperature of approximately 160 K. Chromium films were evaporated on the iron substrate at the slightly elevated temperature of 70 C. Thin iron films were subsequently deposited on these chromium films at room temperature.

RESULTS.

Studies of the clean Fe(001) surface, fig. 2, reveal evidence for a minority spin surface resonance at the center of the zone, approximately 2.7 eV below the Fermi level. As evidenced in fig. 2, the surface designation reflects the sensitivity of the state to adsorption or contamination. Comparison with first principles calculations shows this state to be largely d in character but with some admixture of s and p states [10]. At the center of the zone, where no absolute bandgap exists, the state is essentially a bulk band "resonating" in the surface region. Farther out in the zone, at the X point, a band gap exists and it becomes a surface state. Fig. 3 shows charge density plots for the state at the center and edge of the zone [11], clearly demonstrating the difference in localization between the two points. Although predicted theoretically, no majority counterpart for this state is clearly observed. However the calculations suggest that such a state may possibly be dispersed over a larger range of binding energies.

Deposition of silver on this surface quenches the minority surface peak but a new feature is observed at a lower binding energy [12]. Shown in fig. 4, the latter peak is observed to undergo a maximum in intensity at a silver coverage corresponding to one monolayer, as calibrated by AES. LEED studies of this overlayer system show a good p(1x1) pattern throughout the initial growth. The new peak observed in the photoemission spectrum, fig. 4, is identified with an

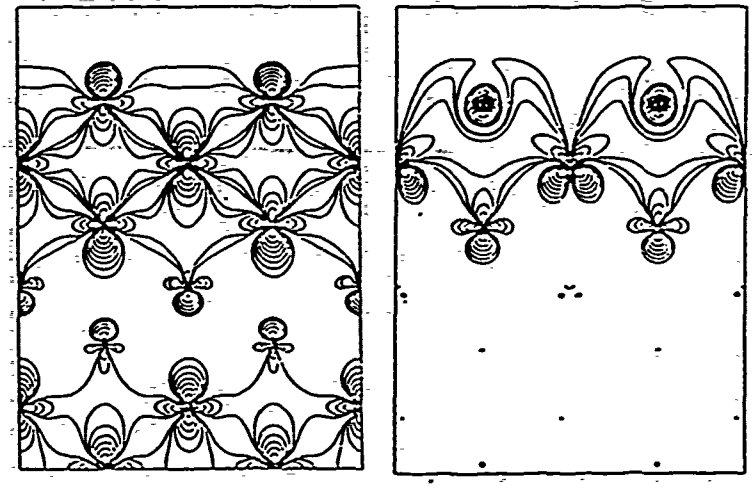

Fig. 3 Calculated charge density plots for the minority surface resonance at the center of the zone and for the same state at the zone boundary where it falls within a bulk band gap

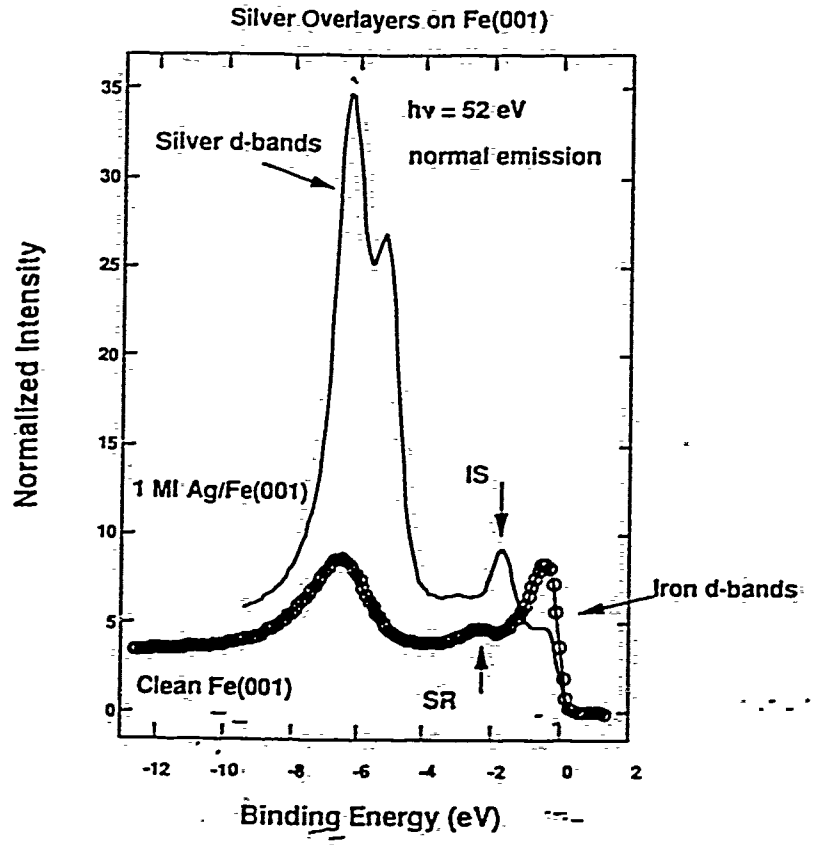

Fig. 4 Photoemission spectrum recorded along the surface normal following the deposition of 1ML of silver on the Fe(001) surface. For comparison the spectrum recorded from the clean surface is also shown. IS indicates the interface state and SR the surface resonanceon the clean surface. Note that the two spectra, both recorded with an incident photon energy of 52 eV, are not normalized with respect to each other.

interface state predicted in a first principles calculations for this overlayer system [13].

With subsequent growth of the silver thin film, the "interface" state is observed to move towards the Fermi level in a series of discrete steps, fig. 5, each step reflecting the layer by layer growth. Spin polarization analysis indicates that in all cases the interface state is of minority spin character [12] and thus suggests that the state is derived from the minority spin surface state observed on the clean surface. The interface state is also observed when an iron monolayer is deposited on a silver (001) surface [14]. However in that case the state is less well resolved and it is not possible to detect any movement reflecting subsequent layers. The experimentally observed dispersion of the Ag/Fe(001) interface state away from the center of the zone is in reasonable accord with the predictions of the calculation [14].

Chromium overlayers deposited on Fe(001) again result in the formation of an interface state derived from the surface state associated with the substrate, fig. 6 [15]. However unlike the silver overlayers the presence of chromium now causes the surface resonance to move further from the Fermi level rather than towards it with the absolute magnitude of the shift being smaller than that observed for silver. The spin integrated spectra of fig. 6 also show an increase in

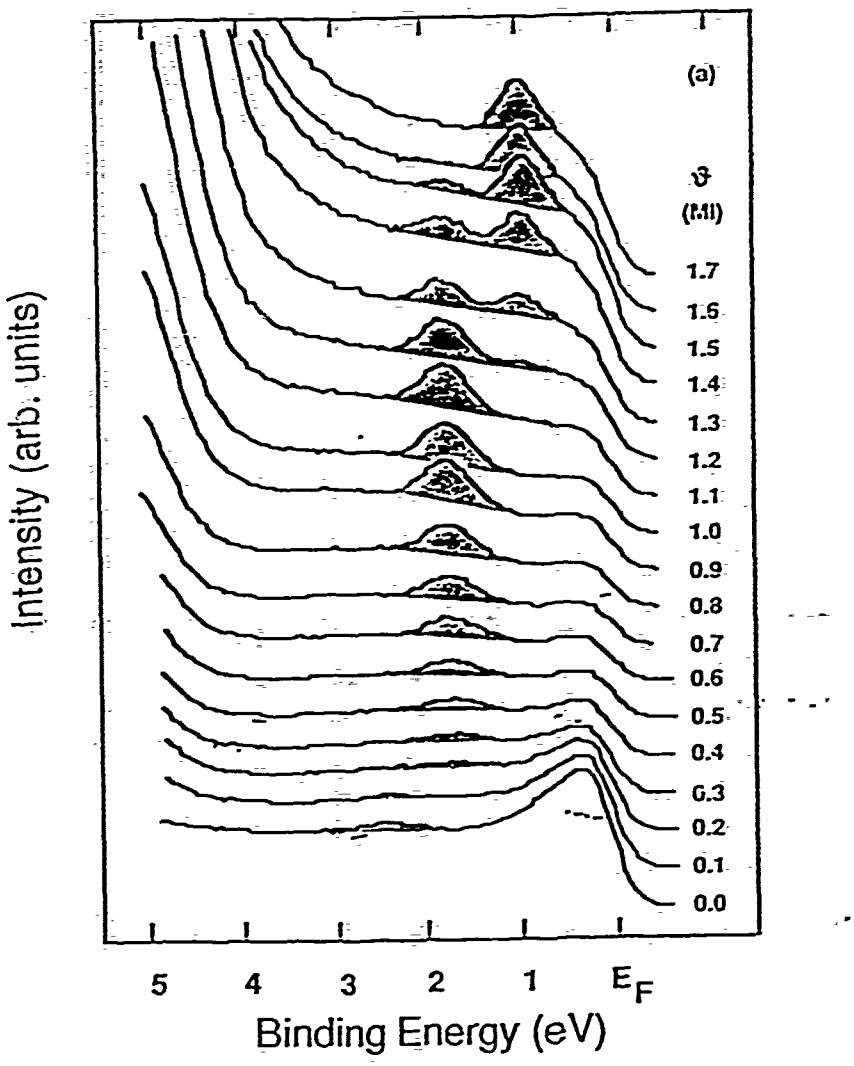

Fig. 5. Photoemission spectra recorded along the surface normal from a series of silver coverages deposited on Fe(001). The different coverages are indicated. The incident photon energy energy is 52 eV and the angle of incidence corresponds to p-polarized light.

the intensity of emission immediately below the Fermi level. A spin polarized spectrum, fig. 7, recorded following the deposition of one monolayer of chromium shows the interface state at a binding energy of 2.7 eV to be entirely of minority spin character, identical to the interface states observed for the silver overlayers. The spin resolved spectrum shows that the new intensity appearing below the Fermi level is also of minority character. Both the spectra in fig.6 and the spectrum in fig.7 are recorded with the light at an angle of incidence corresponding to p polarization. We note that in this photon energy range near the center of the zone a peak below the Fermi level is found in the minority spectrum of clean iron. However in that case, because of the symmetry of the initial state, the intensity is a maximum for s polarized rather than p polarized incident light.

With thicknesses of chromium beyond 2.0 Å the spin integrated spectra in fig. 6 show the evolution of the peak at approximately 3.0 eV binding energy into

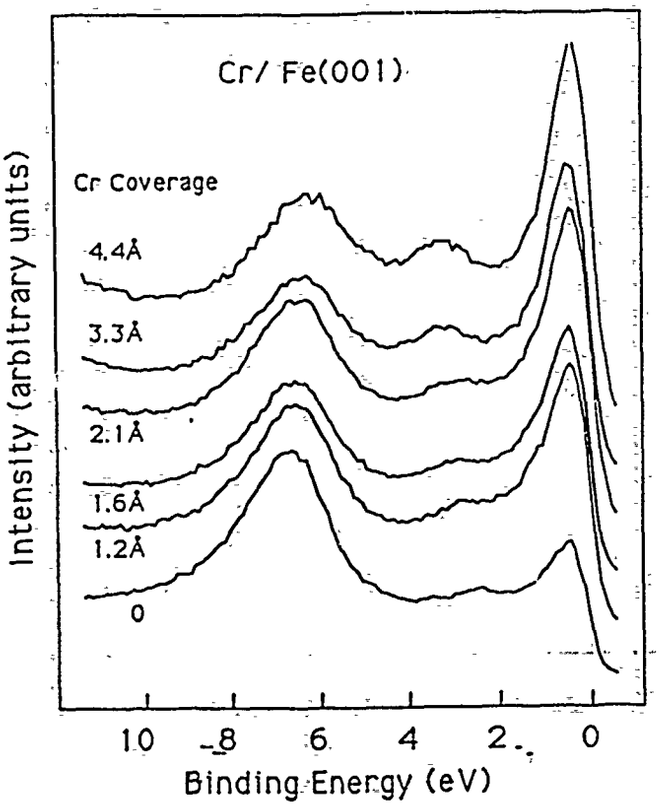

Fig. 6. Spin integrated photoemission spectra recorded from Cr deposited on Fe(001) as a function of Cr coverage. The incident photon energy is 52 eV and the angle of incidence corresponds to p-polarized light.

the chromium surface resonance equivalent to that observed on the clean iron surface. Interestingly, a spin polarized photoemission study of this feature shows no particular polarization indicating that if the Cr(001) surface is ferromagnetic as calculated [16], the presence of steps and terraces masks any possible observation [17].

As noted in the introduction, other experiments have previously shown that iron overlayers deposited on the chromium films may show a parallel or antiparallel magnetic alignment with the iron substrate depending on the thickness of the intervening chromium layer [4]. Figure 7 shows spin resolved photoemission spectra recorded from iron films, 3.3 and 3.9 A thick, grown on chromium films 3.2 and 3.9 A thick, respectively. These spectra clearly show the reversal of polarization associated with the antiparallel alignment on the thicker chromium layer. They also provide some indication that the local moment on the iron for the two systems must be similar in that exchange split counterparts are placed at approximately the same binding energies of 0.5 and 2.5 eV.

DISCUSSION.

The sensitivity to the presence of adsorbates of the minority feature observed in the spin resolved spectra, fig.1, and the close agreement to calculation supports its identification as a surface state. As noted above, the state is a resonance rather than a pure surface state. Such a state is also predicted in a simple tight binding calculation using a nonorthogonal basis set [12]. The latter

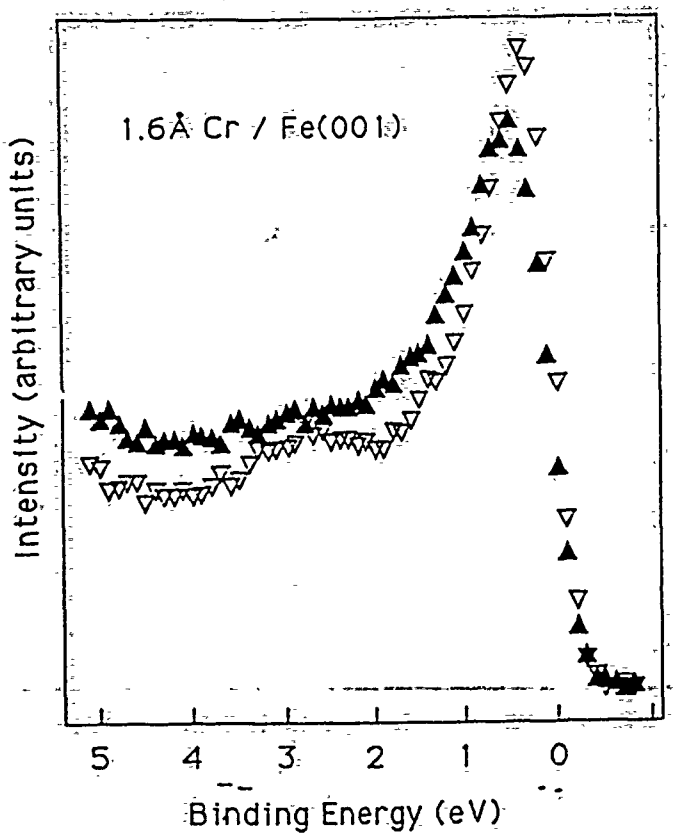

Fig. 7. Spin polarized photoemission spectrum recorded from approximately one monolayer of chromium on Fe(001). The photon energy for this spectrum is 52 eV and the angle of incidence corresponds to p-polarized light.

calculation is a layered scheme with parameters taken from the tabulations, fitted to bulk calculations, provided by Papaconstantopoulos [18]. The modelling was extended to thin overlayers by scaling the respective parameter sets according to the scheme of Andersen [19]. Using such a method a calculation for a silver monolayer on iron (001) found an interface state in close agreement with both experiment and first principles calculation.

The tight binding simulation suggests that with the formation of the interface, a state is formed with 70% of its weight on the surface iron atoms and 30% on the silver monolayer. On the silver side the state has approximately 50% d character, the rest being s and p character. At the same time the modelling indicates that with the formation of the interface, the state becomes more localized within the surface layers of the iron substrate. Thus the decay of the resonant state back into the bulk of the material is reduced. A similar phenomena was previously observed in an inverse photoemission study of an unoccupied interface state in the Nb(110)/palladium interface [20]. In that study it was also shown theoretically that the presence of the palladium tended to localize a niobium surface resonance into the interface region.

Simulations of the chromium monolayer find that, as in the case of silver, the clean iron surface resonance is both localized and shifted by the presence of the overlayer. In agreement with the experiment the interface state is now at a higher rather than lower binding energy. The calculation now finds that the chromium component of the interface state is nearly 80% d in character. This increase in the d component probably reflects the fact, unlike silver, the chromium has unfilled d bands. At the same time the modelling also finds another interface state pulled down below the Fermi level. Unlike the higher binding

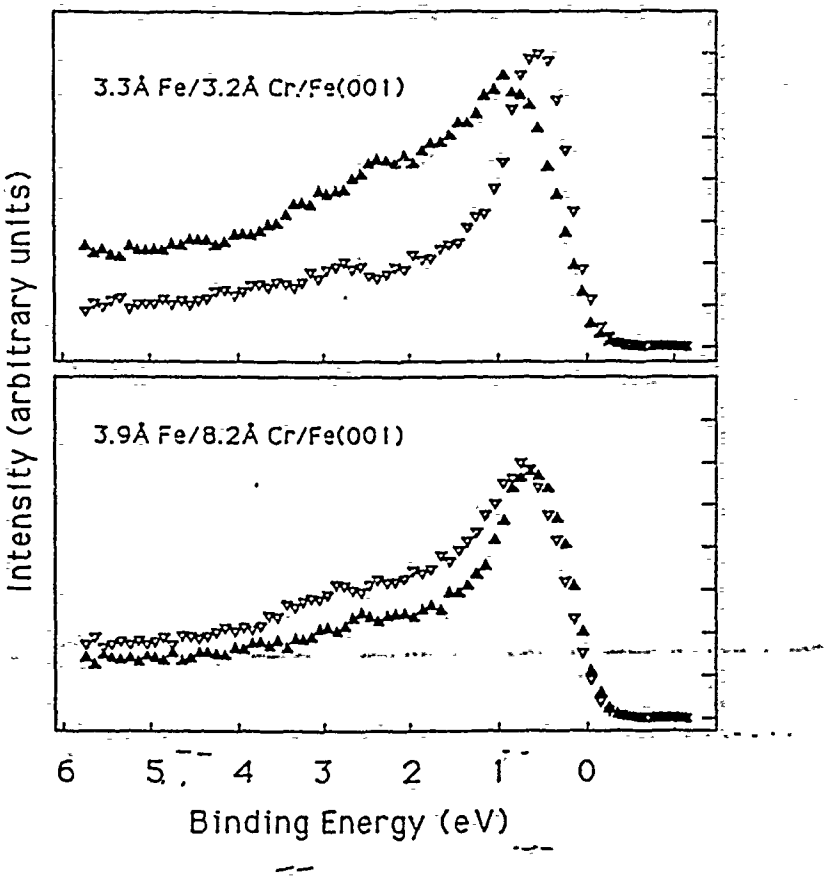

Fig. 8. Spin polarized photoemission spectra recorded from thin iron films of thickness approximately 3.5 Å grown on different thicknesses of chromium. As in previous spectra the photon energy is 52 eV and the angle of incidence corresponds to p-polarized light. The different thicknesses of chromium are indicated in the two panels.

energy interface state, which is d_{z2} in character this second state has d_{xz} character. It is derived from an unoccupied surface state sitting immediately above the Fermi level on the clean iron surface.

To summarize, for both the silver and chromium films the presence of the overlayer appears to localize states within the interface, at least in terms of the decay length into the substrate. These magnetic states, having a well defined spin character, also have weight on the overlayer sites. However it is difficult on the basis of the present experiments to make any quantitative statements regarding the possible existence or size of magnetic moments on the overlayer atoms. In the case of silver, the interface states show well defined binding energies reflecting the thickness of the overlayer film. Thus the presence of the overlayer modifies both the electronic and magnetic properties of the interface. Any modelling that reflects the electronic structure of the interface should allow for the possibility of such changes. One further consideration is the probability of a distinct face dependence for the surface states and surface resonances from which the interface states are derived.

ACKNOWLEDGEMENTS.

The authors of this paper would like to acknowldge many useful discussions with Mike Weinert. This work is supported in part by the U.S. Department of Energy under Contract No. DE-AC02-76CH00016 and in part by the National Science Foundation under Contract No. DMR-86-03304.

REFERENCES.

1. A.J. Freeman, C.L. Fu, S. Ohnishi and M. Weinert, Chapter 1 in "Polarized Electrons in Surface Physics", Ed. by R. Feder, (World Scientific, Singapore 1985).
2. "Magnetism in Ultrathin Films", Special Issue of Appl. Phys. A49, Ed. D. Pescia (1989).
3. L.M. Falicov, D.T. Pierce, S.D. Bader, R. Gronsky, K.B. Hathaway, H.J. Hopster, D.N. Lambeth, S.S.P. Parkin, G. Prinz, M. Salamon, I.K. Schuller and R.H. Victora, J. Mater. Res. 5, 1299 (1990).
4. P. Grunberg, R. Schreiber, Y. Pang, M.B. Brodsky, and H. Sowers, Phys. Rev. Lett. 57,2442 (1986).
5. M.N. Baibich, J.M. Broto, A. Fert, F. Nguyen Van Dau, F. Petroff, P. Etienne, G. Creuzet, A. Friederich, and J. Chazelas,Phys. Rev. Lett. 61,2472 (1986).
6. D.M. Edwards and J. Mathon, to be published.
7. Y. Wang, P.M. Levy and J.L. Fry, Phys. Rev. Lett. 65,2732 (1990).
8. P.D. Johnson, S.L. Hulbert, R. Klaffky, N.B. Brookes, A. Clarke, B. Sinkovic, N.V. Smith, M.J. Kelly, D.T. Pierce, R. Celotta and M.R. Howells, to be published.
9. J. Unguris, D.T. Pierce and R.J. Celotta, Rev. Sci. Inst. 57, 1314 (1986)
10. N. Brookes, A. Clarke, P.D. Johnson and M. Weinert, Phys. Rev. B 41, 2643 (1990).
11. M. Weinert, private communication.
12. N. Brookes, Y. Chang and P.D. Johnson, submitted to Phys. Rev. Lett.
13. S. Ohnishi, M. Weinert and A.J. Freeman, Phys. Rev B 30, 36 (1984).
14. N. Brookes, Y. Chang, P.D. Johnson and M. Weinert, to be published.
15. Y. Chang, N. Brookes and P.D. Johnson, to be published.
16. e.g. P.H. Victora and L.M. Falicov, Phys. Rev B 31, 7335 (1985).
17. S. Blugel, D. Pescia and P.H. Dederichs, Phys. Rev B 39, 1392 (1989); R. Wiesendanger, H.-J. Guntherodt, G. Guntherodt, R.J. Gambino and R. Ruf, Phys. Rev. Lett. 65,247 (1990).
18. D.A. Papaconstantopoulos, "Handbook of the Band Structure of Elemental Solids",(Plenum Press 1986).
19. O.K. Andersen and O. Jepsen, Physica B 91, 317 (1977).
20. X. Pan, P.D. Johnson, M.Wenert, R.E. Watson, J.W. Davenport, G. W. Fernando and S.L. Hulbert, Phys. Rev. B 38, 7850 (1988).

systems. For this purpose, a large number of beam position correcting dipole magnets and coils are installed in the ring. Movements of the experimental photon beams are detected by photon beam position monitors. These signals are used to vary the strengths of the correction dipoles, which steer the positron beam in such a way as to counteract the movement of the synchrotron radiations it emits. This is a very complex system, in which the strengths of some 680 correction dipole magnets and coils are varied at rates up to 100 Hz according to the signals from two sets of photon beam position monitors from each of the beam lines. To do this, the exact transfer functions of the corrector magnets or coils, including the vacuum chamber inside, must be known and taken into account in the design of the feedback circuitry. The breadboard circuitry will be tested on a model system. The logistics and the algorithm for determining the corrections from the deviations are being investigated, formulated in detail, and written as applications programs for the control computer. It is expected that this will be a continuing effort extending even into the operational phase of the completed facility in order to continue improving the stability of the synchrotron radiation x-ray beams as their number increases. □

An APS Prototype Undulator at NSLS

by Jim Viccaro and Efim Gluskin

A new undulator has been installed on the U5 straight section of the VUV ring at the National Synchrotron Light Source (NSLS), Brookhaven National Laboratory. It is a prototype of similar devices planned for the APS. The initial design and specification of the U5 undulator was a collaborative effort between the APS and the Insertion Device Team of the U5 Materials Research Group; the final engineering design and construction was done by Spectra Technology, Inc. of Bellevue, Washington. Some of the pertinent parameters of the device, which has the hybrid magnetic structure, are shown in Table 1.

Using the first and third harmonics, the U5 undulator source will span the photon energy range of approximately 10 to 150 eV. The brilliance of approximately 10^{15} photons/(sec $mm^2 mrad^2$ 0.1%BW), will permit new experiments in such fields as spin-polarized photoemission. In addition, the mechanical structure is unique in that it allows for gap tapers of approximately 10%, which permits control of the band width of the harmonics between approximately one and two times the natural width. This same feature has been requested for the APS. The mechanical structure has a cantilever C-frame design. The magnet array is composed of sections of Nd-Fe-B permanent magnets and vanadium permendur pole pieces. Each section is approximately 0.5-m long; the sections are held on a single-piece aluminum strong-back. The magnets are coated with nickel to prevent deterioration of the magnet block through oxidation. The lower magnet jaw has a spring-loaded mechanism, which compensates for the magnetic and gravitational forces and consequently avoids loading of the drive system in order that a smooth and precise adjustment of the gap is possible over the full operating range of the device. Deflections in the frame associated with the magnetic forces are less than 15 μm at the minimum gap.

Several objectives were addressed in the design of the new device. The first was to incorporate as many mechanical features planned for APS devices as possible to enable us to evaluate their performance. Also, an effort was made to

Table 1. Parameters of the U5 Hybrid Undulator

Magnet Material	Nd-Fe-B
Pole Material	Vanadium Permendur
Period (cm)	7.5
Length (m)	2.3
Minimum Gap (cm)	3.4*
Maximum Field (T)	0.46
Maximum K-Value	3.2
1st Harmonic Tunability (eV)	15 - 50

*The undulator was designed to operate at a minimum of 2.4 cm.

achieve the same degree of field quality and strength so that the brillance and tunability of the device would be close to the theoretical limit. These objectives, which are important for actual APS IDs, had already been met with the short-period APS/CHESS prototype undulator tested on CESR in 1988. In this device, the period length of 3.3 cm permitted the use of single magnet blocks in the construction. In the U5 undulator, however, because of the longer period length, each magnet block is composed of smaller magnets glued together. Both types of construction will be required for APS IDs.

In addition, the requirement of the higher-emittance/low-energy (0.75 GeV NSLS) storage ring on integrated magnetic field moments of IDs are, in fact, very similar to those expected for the low-emittance/high-energy (7 GeV APS) storage ring. These higher moments have a deleterious effect on the stored particle beam and the rather small values require very tight tolerances on the magnetic field of the devices. As can be seen from Table 2, in which both the NSLS and expected APS storage ring requirements are shown, the U5 undulator met or exceeded ***all*** specifications for both rings. Also shown is the excellent field quality achieved for the undulator. It is believed that the rms field error of 0.22% is the smallest achieved for any device installed on a synchrotron.

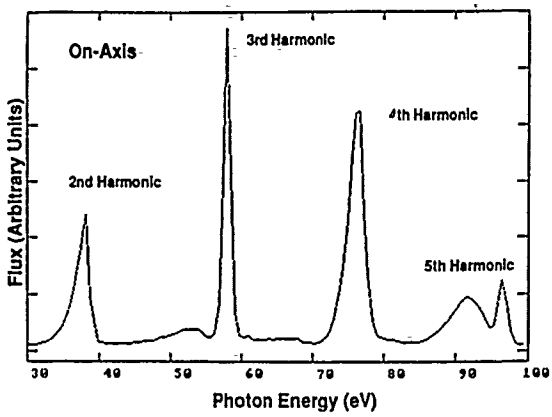

Fig. 1. Photon flux on-axis through a 125 μrad pinhole as a function of photon energy. The K-value is 2.2.

Spectral and storage ring diagnostics are now in progress so that we can completely evaluate the performance of the new undulator. Figure 1 shows some preliminary results for pinhole measurements of the flux. The width of the harmonics shown are within a few percent of the predicted theoretical limit, which is a direct result of the very small field errors of the device. In addition to these measurements, a mapping of the polarization of the device for the harmonics has been performed near 75 eV by means of multilayer mirrors. The results will be made available as soon as the analysis is completed. ❑

Table 2. Magnetic Field Parameters and Storage Ring Requirements

	Specified for NSLS	Measured	Specified for APS
Peak Field (T)	>0.425	0.460	-
$(\Delta B/B)_{rms}$ (%)	<1.0	0.22	0.3
Total Steering Error (G-cm)	<100	13	<100
Integrated Quadrupole (G)	<10	7*	<10
Integrated Sextupole (G/cm)	<100	60*	<100

* At closed gap

Appendix IV

CONFERENCE PROCEEDINGS NO. 236

AMERICAN VACUUM SOCIETY SERIES 12

SERIES EDITOR: GERALD LUCOVSKY
NORTH CAROLINA STATE UNIVERSITY

VACUUM DESIGN OF SYNCHROTRON LIGHT SOURCES

ARGONNE, IL 1990

EDITORS:

YELDEZ G. AMER
SAMUEL D. BADER
ALAN R. KRAUSS
RALPH C. NIEMANN
ARGONNE NATIONAL LABORATORY

AIP
American Institute of Physics New York

L.C. Catalog Card No. 91-55527
ISBN 0-88318-873-2
DOE CONF-901144

Printed in the United States of America.

Contents

Note: The author who delivered the talk is designated by italics.

L.C. Catalog Card No. 91-55527
ISBN 0-88318-873-2
DOE CONF-901144

Printed in the United States of America.

Contents

ADVERTORIAL

VSW Scientific Instruments Ltd. announce a new group catalogue containing their extensive range of Surface Science, Thin Film and Vacuum components. New products include:

The **HAC2000** is a microprocessor controlled analyser control unit. The unit has been designed to operate any of the VSW hemispherical analysers, in the energy range 0 to 2000V; with low noise and fast rise times. Remote computer control is via RS232.

The **EG5000** is a combined medium resolution scanning electron microprobe (SEM) and Auger electron source. Key features include a totally self-contained imaging facility with TV rate and slow scan capability. Fine focussed beams of 5μm diameter, are produced, over the kinetic energy range of up to 5keV.

The **HIB1000** High Resolution EELS sub-system (made under licence from Prof. H. Ibach, KFA-Julich) has achieved the worlds highest reported resolution to date. The EELS system consists of an analyser and monochromator with sophisticated electronics and software. The HIB1000 mounts on a 305mm OD CF flange.

The VSW Reverse View LEED has unparalleled performance in both LEED and Auger applications. The LEED consists of a miniature electron gun, a transparent screen and a 3 or 4 grid optics system; all mounted on a single flange. All parameters may be operated in Local or Remote mode. The unique hand held remote control facility allows the user to adjust the operating parameters whilst viewing the LEED pattern.

Of particular interest to synchrotron users is the development of a true multichannel detection capability for the VSW 50mm mean radius hemispheric anaylser, designed for Angular Resolved Ion and Electron Spectroscopy (ARIES) applications. For further product information contact:

VSW Scientific Instruments Ltd.
Warwick Road South
Old Trafford
Machester
M16 0JT
England

Tel: +44 (0)61 881 6213
Fax: +44 (0)61 881 4624

Circle No. 168

STI OPTRONICS, INC.

- An Amoco Company -

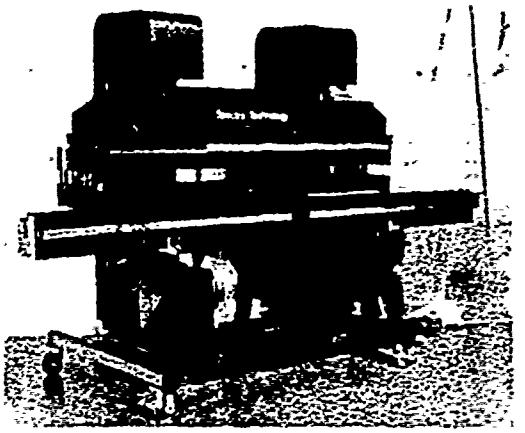

NSLS VUV U-5 Undulator Installed at Brookhaven National Laboratory

Characteristics	
2.3 m	Length
75 mm	Period
34 mm	Min. Gap
4.6 kG	Peak Field

- Production or Custom Designs
- Highest Available Fields with Wedged-Pole Hybrid
- Complete Certification Capability
- Vacuum Chamber and Magnetic Matching to Customer Specifications

STI OPTRONICS, INC.
Tel (206)827-0460,
Fax (206)828-3517
2755 Northup Way,
Bellevue, Washington 98004-1495 USA

Circle No. 164

Appendix VI